Universiteit Antwerpen

This item is the archived peer-reviewed author-version of:

In depth study of transmembrane mucins in association with intestinal barrier dysfunction during the course of T cell transfer and DSS-induced colitis

Reference:
Breugelmans Tom, Van Spaendonk Hanne, de Man Joris, de Schepper Heiko, Jauregui Aranzazu, Macken Elisabeth, Lindén Sara K., Pintelon Isabel, Timmermans Jean-Pierre, De Winter Benedicte, ...- In depth study of transmembrane mucins in association with intestinal barrier dysfunction during the course of T cell transfer and DSS-induced colitis
Journal of Crohn's and colitis - ISSN 1873-9946 - 14:7(2020), jjaa015
Full text (Publisher's DOI): https://doi.org/10.1093/ECCO-JCC/JJAA015
To cite this reference: https://hdl.handle.net/10067/1658740151162165141

uantwerpen.be
Institutional repository IRUA

Manuscript Doi: 10.1093/ecco-jcc/jjaa015

In depth study of transmembrane mucins in association with intestinal barrier dysfunction during the course of T cell transfer and DSS-induced colitis

Tom Breugelmans[1,2,a], Hanne Van Spaendonk[1,2,a], Joris G. De Man[1,2], Heiko U. De Schepper[1,2,3], Aranzazu Jauregui-Amezaga[3], Elisabeth Macken[3], Sara K. Lindén[4], Isabel Pintelon[5], Jean-Pierre Timmermans[5], Benedicte Y. De Winter[1,2,b], Annemieke Smet[1,2,b]

Laboratory of Experimental Medicine and Pediatrics, Faculty of Medicine and Health Sciences, University of Antwerp, Antwerp, Belgium[1]; Infla-Med Research Consortium of Excellence, University of Antwerp, Antwerp, Belgium[2]; Department of Gastroenterology and Hepatology, University Hospital of Antwerp, Antwerp, Belgium[3]; Department of Medical Biochemistry and Cell Biology, University of Gothenburg, Gothenburg, Sweden[4]; Laboratory of Cell Biology & Histology, Department of Veterinary Sciences, University of Antwerp, Antwerp, Belgium[5]

[a] shared first authorship; [b] shared senior authorship

Corresponding author: Annemieke Smet, Laboratory of Experimental Medicine and Pediatrics, Faculty of Medicine and Health Sciences, University of Antwerp, Universiteitsplein 1, 2610, Antwerp, Belgium. Tel: +32 32652611; e-mail: annemieke.smet@uantwerpen.be

Copyright © 2020 European Crohn's and Colitis Organisation (ECCO). Published by Oxford University Press. All rights reserved. For permissions, please email: journals.permissions@oup.com

Accepted Manuscript

Downloaded from https://academic.oup.com/ecco-jcc/advance-article-abstract/doi/10.1093/ecco-jcc/jjaa015/5718468 by Universiteit Antwerpen user on 11 February 2020

Manuscript Doi: 10.1093/ecco-jcc/jjaa015

Part of the work was presented on the following conferences:

ECCO congress 2018, Vienna, Austria

ECCO congress 2019, Copenhagen, Denmark

Belgian Week of Gastroenterology 2018, Antwerp, Belgium

Belgian Week of Gastroenterology 2019, Antwerp, Belgium

Accepted Manuscript

Downloaded from https://academic.oup.com/ecco-jcc/advance-article-abstract/doi/10.1093/ecco-jcc/jjaa015/5718468 by Universiteit Antwerpen user on 11 February 2020

Manuscript Doi: 10.1093/ecco-jcc/jjaa015

Abstract

Background and Aims: There is evidence for a disturbed intestinal barrier function in inflammatory bowel diseases (IBD) but the underlying mechanisms are unclear. Because mucins represent the major components of the mucus barrier and disturbed mucin expression is reported in the colon of IBD patients, we studied the association between mucin expression, inflammation and intestinal permeability in experimental colitis.

Methods: 4 kDa FITC-dextran intestinal permeability and the expression of cytokines, mucins, junctional and polarity proteins were quantified at dedicated time points in the adoptive T cell transfer and DSS-induced colitis models. Mucin expression was also validated in biopsies from IBD patients.

Accepted Manuscript

Downloaded from https://academic.oup.com/ecco-jcc/advance-article-abstract/doi/10.1093/ecco-jcc/jjaa015/5718468 by Universiteit Antwerpen user on 11 February 2020

Manuscript Doi: 10.1093/ecco-jcc/jjaa015

Results: In both animal models, the course of colitis was associated with increased IL-1β and TNF-α expression and increased *Muc1* and *Muc13* expression. In the T cell transfer model, a gradually increasing *Muc1* expression coincided with gradually increasing 4 kDa FITC-dextran intestinal permeability and correlated with enhanced IL-1β expression. In the DSS model, *Muc13* expression coincided with rapidly increased 4 kDa FITC-dextran intestinal permeability and correlated with TNF-α and *Muc1* overexpression. Moreover, a significant association was observed between *Muc1*, *Cldn1*, *Ocln*, *Par3* and *aPKCζ* expression in the T cell transfer model and between *Muc13, Cldn1*, *Jam2*, *Tjp2*, *aPkcζ*, *Crb3* and *Scrib* expression in the DSS model. Additionally, *MUC1* and *MUC13* expression was upregulated in inflamed mucosa of IBD patients.

Conclusions: Aberrantly expressed Muc1 and Muc13 might be involved in intestinal barrier dysfunction upon inflammation by affecting junctional and cell polarity proteins, indicating their potential as therapeutic targets in IBD.

Keywords

T cell transfer and DSS-induced colitis mouse models; Muc1 and Muc13; intestinal mucosal barrier dysfunction

Accepted Manuscript

Downloaded from https://academic.oup.com/ecco-jcc/advance-article-abstract/doi/10.1093/ecco-jcc/jjaa015/5718468 by Universiteit Antwerpen user on 11 February 2020

Manuscript Doi: 10.1093/ecco-jcc/jjaa015

1. Introduction

Inflammatory bowel diseases (IBD), including Crohn's disease (CD) and ulcerative colitis (UC), remain disease entities with a high morbidity burden and are characterized by perpetual chronic relapsing inflammation of the intestines[1]. At this moment, there is no curative treatment for IBD, which is why patients require life-long medication and often need surgery[2]. Treatment mainly focuses on immunosuppression and still a substantial number of patients fail to respond or obtain full remission[3].

The etiology and pathogenesis of IBD are believed to involve inappropriate immune responses to the complex microbial flora in the gut in genetically predisposed persons. The intestinal mucosal barrier separates the luminal content from host tissues and plays a pivotal role in the communication between the microbial flora and the mucosal immune system. Emerging evidence suggests that loss of barrier integrity, also referred to 'leaky gut', is a significant contributor to the pathophysiology of IBD[4,5]. The intestinal mucosal barrier comprises a thick layer of mucus, a single layer of epithelial cells and the lamina propria hosting innate and adaptive immune cells. Integrity of this barrier is maintained in several ways as depicted in Figure 1. Secreted (e.g. MUC2) and transmembrane (e.g. MUC1, MUC4, MUC13) mucins represent the major components of the mucus barrier and are characterized by domains rich in proline, threonine, and serine that are heavily glycosylated (i.e. PTS domains). In addition to having a protective function, transmembrane mucins possess extracellular EGF-like domains and intracellular phosphorylation sites which enable them to also participate in the intracellular signal transduction. In this way, they can modulate intestinal inflammation by affecting epithelial cell proliferation, survival, differentiation and cell-cell interactions[6,7].

The intestinal epithelium underneath the mucus layer plays an active role in innate immunity via the secretion and expression of mucins and antimicrobial peptides as well as by hosting antigen

Accepted Manuscript

Downloaded from https://academic.oup.com/ecco-jcc/advance-article-abstract/doi/10.1093/ecco-jcc/jjaa015/5718468 by Universiteit Antwerpen user on 11 February 2020

presenting cells. At this level, intense communication takes place between intestinal epithelial cells (IECs), immune cells, the microbiome and environmental antigens shaping immune responses towards tolerance or activation[8]. IECs are mechanically tied to one another and are constantly renewed to maintain proper barrier function[9]. This linkage is achieved by three types of intercellular junctions, listed from the apical to basal direction: tight junctions, adherens junctions and desmosomes[10]. Whereas the adherens junctions and desmosomes are essential to maintain cell-cell adhesion by providing mechanical strength to the epithelium, tight junctions regulate paracellular permeability and seal the intestinal barrier. Tight junctions mainly consist of claudins (CLDNs), occludin (OCLN), tricellulin and junctional adhesion molecules (JAMs). Apart from linking neighbouring cells, they associate with peripheral intracellular membrane proteins, such as zonula occludens (ZO) proteins, which anchor them to the actin cytoskeleton[10,11]. Furthermore, tight junctions are also involved in regulating cell polarity which is established by the mutual interaction of three evolutionary conserved complexes: defective partitioning (PAR; PAR3 – PAR6 – aPKC), Crumbs (CRB3 – PALS1 – PATJ) and Scribble (SCRIB – DLG – LGL) complexes (Figure 1). The Crumbs complex defines the apical membrane whereas the PAR and Scribble complexes are responsible for the establishment of the apical-lateral junctions between cells and the basolateral membrane, respectively[12,13,14]. These polarity complexes are thus complementary and act together to initiate and maintain apical-basal polarity[5,15].

Mouse models of colitis have been major tools in investigating alterations in the intestinal mucosal barrier during the course of IBD, yet most of these studies have been concentrated on measuring a restricted spectrum of parameters, i.e. analyzing either changes in barrier integrity characterized by tight junction dysfunction or changes in mucin expression upon inflammation[5,16–23]. To date, the association between aberrant mucin expression and the altered function of the intestinal mucosal barrier in IBD remains largely unexplored. It has been shown that Muc2 is critical for colonic

Accepted Manuscript

Downloaded from https://academic.oup.com/ecco-jcc/advance-article-abstract/doi/10.1093/ecco-jcc/jjaa015/5718468 by Universiteit Antwerpen user on 11 February 2020

protection as mice lacking this secretory mucin develop severe colitis[24]. Furthermore, Muc1 and Muc13 are significantly increased in expression in the intestinal mucosae of colitis mice[25,26]. During acute inflammation, these transmembrane mucins inhibit epithelial cell apoptosis in the gastrointestinal tract[26,27]. Nevertheless, aberrant changes in their expression pattern upon chronic inflammation could lower the level of protection concerning the intestinal epithelium. More specifically, inappropriate overexpression of transmembrane mucins could affect barrier integrity by modulating apical-basal cell polarity and cell-cell interactions, resulting in tight junction dysfunction, and may thus be responsible for the progression from local inflammation to more severe diseases, including IBD[6,28,29]. Therefore, in order to enhance our understanding of the role of transmembrane mucins as novel players in intestinal mucosal barrier dysfunction in IBD, we conducted an *in vivo* study to characterize changes in barrier components affecting integrity during the course of colitis using two complementary mouse models.

Accepted Manuscript

Downloaded from https://academic.oup.com/ecco-jcc/advance-article-abstract/doi/10.1093/ecco-jcc/jjaa015/5718468 by Universiteit Antwerpen user on 11 February 2020

Manuscript Doi: 10.1093/ecco-jcc/jjaa015

2. Material and Methods

2.1. Animals

Eight- to nine-week-old female immunocompromised SCID (C.B-17/Icr-*Prkdc*^{scid}/IcrIcoCrl) and BALB/c mice (T cell transfer model) and 7- to 8-week-old male C57BL/6J mice (DSS model) were purchased from Charles River (France). All animals were housed in a conventional animal facility with ad libitum access to food and water and a light cycle of 12 hours. After arrival in the animal facility, mice were allowed to acclimatize for 7 days before the onset of the experiments. All experiments were approved by the Ethical Committee for animal experimentation of the University of Antwerp, Belgium (ECD-file 2014-42 (T cell transfer model), ECD-file 2017-43 (DSS model)).

2.2. Colitis models and experimental design

Mouse models are essential tools to understand IBD pathogenesis, yet each separate model has its limitations in that it not fully recapitulates the complexity of this human disease[4,30]. Among these, the adoptive T cell transfer model has mainly been used to investigate the immunological mechanisms of intestinal inflammation mediated by T cells, and to a lesser extent to study barrier integrity. By contrast, the dextran sodium sulphate (DSS) model has been described as a useful model to examine the innate immune mechanisms involved in the development of intestinal inflammation and barrier dysfunction. More specifically, DSS is toxic to the colonic epithelium and oral administration of this chemical compound causes epithelial cell injury and innate immune responses which alter mucosal barrier integrity[23,31]. As each colitis model provides valuable insights into a certain aspect of IBD, using multiple models will thus yield a broader picture of the pathophysiology of these diseases, including barrier dysfunction.

Accepted Manuscript

Downloaded from https://academic.oup.com/ecco-jcc/advance-article-abstract/doi/10.1093/ecco-jcc/jjaa015/5718468 by Universiteit Antwerpen user on 11 February 2020

T-cell transfer model: colitis was induced in SCID mice by the adoptive transfer of $CD4^+$ $CD25^-$ $CD62L^+$ T cells isolated from the spleens of BALB/c donor mice as described before (Supplementary Figure S1A)[32]. To monitor disease progression, animals were weighed every week and clinically scored based on the following clinical disease parameters: weight loss, piloerection, stool consistency and mobility. Each parameter was graded from 0 to 2 according to disease severity (0 = absent, 1 = moderate, 2 = severe; for weight loss, 0 = weight gain, 1 = stable, 2 = weight loss). The cumulative score hence ranged from 0 to 8. In addition, intestinal inflammation was also monitored in a continuous manner in individual mice by colonoscopy at fixed time points (weeks 0, 2, 4 and 6) using a flexible Olympus URF type P5 ureteroscope with an outer diameter of 3.0 mm (Olympus Europe GmbH)[33]. Briefly, mice were sedated with a mixture of ketamine (60mg/kg, Ketalar, Pfizer) and xylazine (6.67 mg/kg, Rompun, Bayer) (intraperitoneally (i.p.)) and placed in prone position. The anal sphincter was lubricated with gel (RMS-endoscopy) to facilitate insertion of the endoscope. Subsequently, the scope was carefully inserted through the anus as far as possible into the colon of the sedated mouse. A score was given during the withdrawal of the scope for the following parameters: morphology of the vascular pattern, bowel wall translucency, fibrin attachment and presence of loose stools (each ranging from 0 to 3), with a cumulative minimum of 0 (no inflammation) and a maximum of 12 (severe inflammation).

DSS-induced colitis model: acute colitis was induced by administering 2% DSS (36-50 kDa) to autoclaved drinking water for 7 days ad libitum. This cycle was repeated two more times with intermediate recovery phases of normal drinking water for 7 days to induce more chronic forms of colitis. Control mice received only autoclaved drinking water (Supplementary Figure S2A). Water levels were checked every day and were refreshed every other day. Each day, an individual disease activity index (DAI) was calculated by analysing weight loss (0 = <1%, 1 = 1-5%, 2 = 5-10%, 3 = 10-20%, 4 = >20%), stool consistency (0 = normal, 1 = semi-solid, 2 = loose stools, 4 = diarrhea) and

Accepted Manuscript

Downloaded from https://academic.oup.com/ecco-jcc/advance-article-abstract/doi/10.1093/ecco-jcc/jjaa015/5718468 by Universiteit Antwerpen user on 11 February 2020

rectal bleeding (0 = no bleeding, 2 = blood visible, 4 = gross bleeding) to obtain a cumulative score of these parameters ranging from 0 (healthy) to 12 (severe colitis).

At 1, 2, 4 and 6 weeks post-transfer and at the end of each DSS treatment (Supplementary Figure S1A & S2A), 10-14 animals per group (control, T cell transfer and DSS) were sacrificed by exsanguination under anesthesia (90 mg/kg ketamine and 10 mg/kg xylazine; i.p.). The collected blood was centrifuged to obtain serum for further analysis. Subsequently, the colon was resected, feces were removed and the weight as well as the length of the colon were determined and expressed as the weight/length ratio (mg/cm). Macroscopic inflammation was then scored based on the following parameters: presence of ulcerations, hyperemia, bowel wall thickening and mucosal edema. For the T cell transfer model, each parameter was scored from 0 to 3 depending on the severity, leading to a maximum cumulative score of 12 as described by Heylen *et al.*[33]. For the DSS model, the macroscopic scoring system of Wallace *et al.* was used resulting in a score from 0 to 5[34]. Thereafter, different samples from the colon (distal side) were taken and processed immediately or stored in RNA later, snap frozen or embedded in paraffin or cryoprotectant until further analysis (see below).

2.3. IBD patients and clinical specimens

IBD patients that underwent an endoscopy for clinical reasons (i.e. follow-up of disease remission or the presence of an acute flare), were recruited via the policlinic of the University Hospital of Antwerp (UZA), Belgium. Colonic biopsies were collected from 13 patients with active disease (6 CD, 7 UC) and 15 patients in remission (10 CD, 5 UC) and stored in RNA later at -80°C until further use. All patients were previously diagnosed with IBD based on complaints, blood and stool tests, radiography, endoscopy and histology. Disease activity was mainly based on the presence of active

Accepted Manuscript

Downloaded from https://academic.oup.com/ecco-jcc/advance-article-abstract/doi/10.1093/ecco-jcc/jjaa015/5718468 by Universiteit Antwerpen user on 11 February 2020

symptoms and endoscopic and microscopic evaluation of the colon. Prior to endoscopy, informed consent from each patient was obtained. This study was approved by the Ethical Committee of the UZA (Belgian Registration number B300201733423).

2.4. *In vitro* cell culture assay

LS513 cells (human colorectal carcinoma (ATCC© CRL-2134™)) were sustained in RPMI-1640 medium (Life Technologies) supplemented with 10% heat-inactivated fetal calf serum, 100 U/ml penicillin, 100 µg/ml streptomycin, and 2mM L-glutamine. LS513 cells were seeded and grown in 6 well-plates (1 x 10^6 cells/ml). After reaching confluence, the cells were treated with 40 ng/ml TNF-α or IL-1β for 24 hours. Untreated cells were included as controls. Thereafter, cells were lysed for RNA extraction purposes. Three independent experiments were performed containing 3 technical replicates for each condition.

2.5. Myeloperoxidase (MPO) activity assay

Myeloperoxidase (MPO) activity was measured in colonic tissue as a parameter for neutrophil infiltration[33,35,36]. Briefly, colonic samples were immersed in potassium phosphate (pH 6.0) containing 0.5% hexadecyltrimethylammonium bromide (0.02 mL/mg tissue). Thereafter, samples were homogenized, subjected to two freeze-thawing cycles and subsequently centrifuged at 15000 rpm for 15 min at 4°C. An aliquot (0.1 mL) of the supernatant was then added to 2.9 mL of o-dianisidine solution (i.e. 16.7 mg of o-dianosidine dihydrochloride in 1 mL of methyl alcohol, 98 mL of 50 mM potassium phosphate buffer at pH 6.0 and 1 mL of 0.005% H_2O_2 solution). Immediately afterwards, the change in absorbance of the samples was read at 460 nm over 60 sec using a Spectronic Genesys 5 spectrophotometer (Milton Roy). One unit of MPO activity equals the amount of enzyme able to convert 1 mmol of H_2O_2 to H_2O per min at 25°C.

Accepted Manuscript

Downloaded from https://academic.oup.com/ecco-jcc/advance-article-abstract/doi/10.1093/ecco-jcc/jjaa015/5718468 by Universiteit Antwerpen user on 11 February 2020

Downloaded from https://academic.oup.com/ecco-jcc/advance-article-abstract/doi/10.1093/ecco-jcc/jjaa015/5718468 by Universiteit Antwerpen user on 11 February 2020

2.6. RNA extraction and RT-qPCR for gene expression

Total RNA from murine and human colonic tissue stored in RNA later and from collected LS513 cells, was extracted using the NucleoSpin® RNA plus kit (Macherey-Nagel) following the manufacturer's instructions. The concentration and quality of the RNA were evaluated using the NanoDrop® ND-1000 UV-Vis Spectrophotometer (Thermo Fisher Scientific). Subsequently, 1 µg RNA was converted to cDNA by reverse transcription using the SensiFast™ cDNA synthesis kit (Bioline). Relative gene expression was then determined by SYBR Green RT-qPCR using the GoTaq qPCR master mix (Promega) on a QuantStudio 3 Real-Time PCR instrument (Thermo Fisher Scientific). Primer sequences are shown in supplementary Table S1. All RT-qPCR reactions were performed in duplicate and involved an initial DNA polymerase activation step for 2 min at 95°C, followed by 40 cycles of denaturation at 95°C for 15 sec and annealing/extension for 1 min at 60°C. Analysis and quality control were performed using qbase+ software (Biogazelle). Relative expression of the target genes was normalized to the expression of the housekeeping genes *Actb* and *Rpl4* (for the murine samples) and *ACTB* and *GAPDH* (for the human samples).

2.7. Quantification of intestinal permeability

To assess *in vivo* intestinal permeability, the FITC-dextran intestinal permeability assay was performed as described by Gupta *et al.*[37]. In brief, mice were intragastrically inoculated 4 hours prior to euthanasia with FITC-dextran (44 mg/100 g body weight (T cell transfer), 60 mg/100 g body weight (DSS model), 4 kDa, Sigma). Upon euthanasia, blood was collected via cardiac puncture and transferred into SSTII Advance Blood Collection Tubes (BD Vacutainer). After centrifugation (10000 rpm, 5 min), serum was collected and equally diluted with PBS. Subsequently, aliquots of 100 µl were added in duplo to a 96-well microplate and the concentration of FITC was measured by spectrophotofluorometry (Fluoroskan Microplate Fluorometer, Thermo Fisher Scientific) at an

Accepted Manuscript

excitation wavelength of 480 nm and an emission wavelength of 530 nm. The exact FITC-dextran concentration per well was calculated using a standard curve with serially diluted FITC-dextran solutions.

2.8. Cytokine measurements

To determine colonic inflammatory mediators at protein level, two different approaches were applied.

First, fresh colonic segments were rinsed with PBS, blotted dry and weighed. Subsequently, the samples were stored on ice until further processing in a Tris-EDTA buffer (i.e. PBS containing 10 mM Tris, 1 mM EDTA, 0.5% *v/v* Tween-20 and a protease-inhibitor cocktail (Sigma-Aldrich)) at a ratio of 100 mg tissue per ml buffer. Samples were then homogenized, centrifuged (11 000 rpm, 10 min, 4°C) and the supernatants were stored at -80°C until further analysis. Colonic cytokine levels were quantified using cytometric bead arrays (CBA) (BD Biosciences) for Tumour Necrosis Factor (TNF)-α, Interferon (IFN)-γ, Interleukin (IL)-1β and IL-6 according to the manufacturer's instructions. Fluorescence detection was performed on a BD Accuri C6 flow cytometer and the FCAP Array software was used for data analysis.

Second, snap frozen colonic tissues were homogenized using beads and total protein was extracted in ice cold NP-40 buffer (i.e. 20 mM Tris HCl (pH 8.0), 137 mM NaCl, 10% glycerol, 1% nonidet-40, 2 mM EDTA) supplemented with protease and phosphatase inhibitor cocktail tablets (Roche). After centrifugation (14.000 rpm, 10 min, 4°C) to remove cell debris, the protein concentration was determined using the Pierce BCA protein assay kit (Thermo Fisher Scientific). Enzyme-Linked ImmunoSorbent Assay (ELISA) was then performed to quantify colonic cytokine expression at the protein level. To this end, the mouse uncoated ELISA kits (Invitrogen) were used according to the manufacturer's instructions to measure protein concentrations of IL-1β, TNF-α, IL-6, IL-10 and IL-22.

Accepted Manuscript

Downloaded from https://academic.oup.com/ecco-jcc/advance-article-abstract/doi/10.1093/ecco-jcc/jjaa015/5718468 by Universiteit Antwerpen user on 11 February 2020

A standard curve was created by performing 2-fold serial dilutions of the top standards included in the kits. For each sample, 100µl of a 2.5 µg/ml protein solution was analysed by ELISA in duplicate.

2.9. Quantification of mucin protein expression by Western Blotting

Ten µg of protein extracted from murine colonic tissue in ice cold NP-40 buffer (supplemented with Protease and Phosphatase Inhibitor Cocktail Tablets) was diluted in 2x Laemmli buffer (Bio-Rad) supplemented with 5% β-mercaptoethanol, boiled for 5 minutes and loaded on NuPAGE 12% Bis-Tris Protein Gels (Invitrogen). Protein separation was performed by gel electrophoresis in 1x MOPS Running buffer. Total protein was transferred onto a Immobilon-FL PVDF Membrane (Millipore), which was blocked for 1 hour using 1:5 Odyssey Blocking Buffer (Li-Cor) in PBS. The blots were incubated overnight at 4°C with the following primary antibodies: MUC1 (ab80952 (abcam), 1/1000), in-house MUC13 (1/500) and β-actin (1/20 000, for normalization of relative protein expression). MUC13 and β-actin expression was visualised using infrared target detection, by incubating the blots for 1 hour at room temperature with IRDye 800CW Goat anti-Mouse (926-32210, Li-Cor) and IRDye 680RD Goat anti-Rabbit (926-68071, Li-Cor) secondary antibodies. MUC1 expression was evaluated by chemiluminescent detection by incubating the blots for 1 hour with a biotynilated goat anti-armenian hamster secondary antibody (1/200, Vector Laboratories), after which avidin-biotin-HRP complexes were added and chemoluminescence was detected using the SuperSignal West Femto Maximum Sensitivity Substrate (Thermo Scientific). Washing steps were performed using PBS supplemented with 0.1% Tween. The Odyssey Imaging system (Li-Cor), the Li-Cor Image studio v4.0 Software and ChemiDoc Touch imaging Software (Bio-Rad) were used for blot visualisation and protein quantification.

Accepted Manuscript

Downloaded from https://academic.oup.com/ecco-jcc/advance-article-abstract/doi/10.1093/ecco-jcc/jjaa015/5718468 by Universiteit Antwerpen user on 11 February 2020

Manuscript Doi: 10.1093/ecco-jcc/jjaa015

2.10. Histopathology and immunohistochemistry

In order to evaluate inflammation at the microscopic level, full thickness colonic segments were fixed for 24 h in 4% formaldehyde and subsequently embedded in paraffin. Cross sections (5 µm thick) were deparaffinized and rehydrated. Sections were then stained with Hematoxylin Gill III Prosan (Merck) and Eosin Yellow (VWR) according to the standardized protocols. Inflammation was scored based on the degree of inflammatory infiltrates (0-3), presence of goblet cells (0-1), crypt architecture (0-3), mucosal erosion and/or ulceration (0-2), presence of crypt abscesses (0-1) and the number of layers affected (0-3), resulting in a cumulative score ranging from 0 to 13[35]. Periodic Acid-Schiff (PAS) staining was performed to detect mucin glycoproteins in paraffin-embedded colon sections. In brief, rehydrated 5 µm thick colon sections were placed in Schiff reagent for 15 min after an initial oxidation step in 0.5% periodic acid solution for 5 min. Then, colon sections were washed with tap water, counterstained with hematoxylin and analysed by light microscopy (Olympus BX43).

Several immunohistochemical stainings were also applied on paraffin-embedded colonic tissue using the following primary antibodies: the polyclonal rabbit Muc1 (Abcam (ab15481), 1/1000), Muc2 (Novus Biologicals (NBP1-31231), 1/3000), Muc4 (Novus Biologicals (NBP1-52193SS), 1/3000), the in-house Muc13 (1/2000) and SCRIB (Invitrogen (PA5-28628, 1/500) antibodies. Briefly, heat-induced antigen retrieval was performed in EDTA (pH 8) (MUC1 and MUC13) or citrate buffer (10 mM, pH 6) (MUC2, MUC4, PAR3 and SCRIB). Subsequently, and solely for the mucin stainings, endogenous peroxidase activity was blocked by incubating the slides with 3% H_2O_2 in methanol (5 min). Primary antibody incubation was performed overnight at 4°C (MUC1, MUC2, MUC4 and MUC13) or at room temperature (SCRIB). The mucins were visualized by incubating the colon sections with a goat anti-rabbit biotinylated secondary antibody (EnVision detection system for MUC13) for 60 min at room temperature, followed by incubation with HRP-avidin complexes. Finally, visualization of the target antigen was performed by a short incubation with aminoethyl carbazole (AEC), after which the sections were counterstained with hematoxylin and analysed by light microscopy (Nikon Eclipse Ti inverted microscope) and ImageJ software. For the visualization of the SCRIB cell polarity protein,

Accepted Manuscript

Downloaded from https://academic.oup.com/ecco-jcc/advance-article-abstract/doi/10.1093/ecco-jcc/jjaa015/5718468 by Universiteit Antwerpen user on 11 February 2020

the colon sections were incubated with a Goat Anti-Rabbit Cy3 antibody (1/500) for 2 hours and counterstained with DAPI. By using confocal laser scanning microscopy (Leica TCS SP8 X microscope), both maximal intensity projections of confocal z-stack images and detailed single confocal plane images zooming in on several epithelial cells were generated.

To visualize tight junctions in the colon, fresh colonic tissue was transversally placed and immersed in Richard-Allan Scientific™ Neg-50™ Frozen Section Medium (Thermo Fisher Scientific) and snap frozen, after which 6 µm cryosections were mounted on SuperFrost slides (Thermo Fisher Scientific). After a short fixation period of 5 min in aceton, the sections were dried and rinsed with Tris-buffered saline supplemented with 1% albumin. The sections were then incubated overnight with the following primary antibodies: ZO-1 (Invitrogen (61-7300), 1/1000) and CLDN1 (abcam (ab15098), 1/2000). The next day, secondary antibody incubation was performed for 60 min using a goat anti-rabbit Alexa Fluor 594 secondary antibody (Invitrogen, 1/800). After rinsing in distilled water, the colon sections were counterstained and protected against fading using Vectashield mounting medium containing DAPI (Vector Laboratories). Washing steps were performed using Tris-buffered saline supplemented with 0.1% Triton X-100. For visualization, maximal intensity projections of confocal z-stack images were generated by confocal laser scanning microscopy (Leica TCS SP8 X microscope). Furthermore, detailed single confocal plane images of tangentially-sectioned and cross-sectioned cells were also included to highlight the subcellular localization.

2.11. Statistics

Statistical analysis using the GraphPad Prism 8.00 software (licence DFG170003) was performed to determine significant differences between different experimental groups (control and the different colitis groups within a certain model (T cell transfer or DSS), untreated versus cytokine-stimulated LS513 cells, inflamed and non-inflamed colonic tissue from IBD patients). Data from the experimental colitis models and cell culture assays were analysed by the One-way Analysis of Variance (ANOVA) and non-parametric Kruskal-Wallis tests and are presented as means ± standard

Accepted Manuscript

Downloaded from https://academic.oup.com/ecco-jcc/advance-article-abstract/doi/10.1093/ecco-jcc/jjaa015/5718468 by Universiteit Antwerpen user on 11 February 2020

error of mean (SEM) or boxplots (min to max), unless stated otherwise. Significance levels are indicated on the graphs by *p<0.05, **<0.01, ***p<0.001 and were corrected for multiple testing using the Tukey-Kramer's and Dunn's post-hoc multiple comparisons tests. Data obtained from human IBD patients was statistically evaluated using the Wilcoxon matched-pairs signed-rank test (inflamed versus non-inflamed tissue in patients with active IBD) and the Mann-Whitney U test (patients with active IBD versus patients in remission). Statistical testing between the different IBD subtypes was performed by using the Kruskal-Wallis test with Dunn's post-hoc multiple comparison test.

A discriminant function analysis was performed to determine whether colitis mice could be distinguished from control animals based on a set of predictor variables (i.e. the expression of cytokines, mucins or other barrier mediators). The results are depicted as scatter plots showing the two main discriminant functions (i.e. function 1 and function 2) with the according main predictor variables summarized in a table. Furthermore, a multiple linear regression analysis was carried out to investigate associations (1) between changes in barrier integrity and the expression of mucins and cytokines; (2) between the expression of mucins, cytokines and barrier mediators. Scatter plots are shown distinguishing between different experimental groups with the corresponding R^2- and p-value of the regression model. A p-value below 0.05 was considered statistically significant. These analyses were performed using IBM SPSS Statistics 24 software.

Accepted Manuscript

3. Results

3.1. Macroscopic and microscopic observations of colitis evolution over time

In the **T cell transfer model**, SCID mice started to develop clinical signs of colitis one week after the adoptive transfer of naïve T cells. Body weight was decreased at 1 week post-transfer compared to

Downloaded from https://academic.oup.com/ecco-jcc/advance-article-abstract/doi/10.1093/ecco-jcc/jjaa015/5718468 by Universiteit Antwerpen user on 11 February 2020

the initial body weight pre-transfer and this decrease gradually continued until week 6 (Supplementary Figure S1B). The clinical disease score increased over time starting from week 1 to week 4, while stagnating afterwards (Supplementary Figure S1C). A colonoscopy was performed every 2 weeks to monitor signs of colitis in the bowel wall, with higher scores seen at weeks 2, 4 and 6 post-transfer compared to the control mice (Supplementary Figure S1D). After sacrifice, the mucosal damage in the colon was scored at both a macro- and microscopic level. Mice that were sacrificed at 2, 4 and 6 weeks post-transfer showed an increase in macroscopic inflammation (Supplementary Figure S1E). This phenomenon was also seen for another macroscopic marker of colonic inflammation, the colonic weight/length ratio, which is a quantification of colonic edema (Supplementary Figure S1F). In contrast, the infiltration of neutrophils and lymphocytes became already visible on H&E-stained colonic segments of colitis mice at week 1 post-transfer (Supplementary Figure S1G & I). This mucosal and submucosal infiltration of immune cells gradually increased and was associated with a remarkable increase in colon thickness as disease progressed to weeks 2, 4 and 6 (Supplementary Figure S1G & I). Furthermore, MPO activity, which is caused by neutrophil infiltration in the mucosa, was increased starting from 2 weeks post-transfer, with a gradual increase over time to weeks 4 and 6 (Supplementary Figure S1H).

In the **DSS colitis model**, mice treated with DSS started to lose weight after 5 days of DSS administration in the first cycle. The body weight further decreased when normal drinking water was reintroduced at day 8, with a maximal weight loss at day 11 of the experimental protocol (Supplementary Figure S2B). The colitis mice started to regain weight at the end of the second DSS cycle (day 21) until the initial body weight was reached at the end of the experiment. Healthy control mice gained weight over time (Supplementary Figure S2B). As a result of DSS administration, mice in each DSS group showed maximal changes in stool consistency and rectal bleeding after 7 days of DSS administration, which decreased and completely disappeared in the recovery phase (Supplementary Figures S2C-D). The above-described parameters to assess clinical disease in this model (body weight, stool consistency and rectal bleeding) are combined in the DAI score, which is shown in

Accepted Manuscript

Downloaded from https://academic.oup.com/ecco-jcc/advance-article-abstract/doi/10.1093/ecco-jcc/jjaa015/5718468 by Universiteit Antwerpen user on 11 February 2020

Supplementary Figure S2E. Control mice did not show any signs of disease throughout the experiment, whereas administration of 2% DSS for 7 days stably induced a mild acute colitis. The two subsequent DSS cycles, however, led to the development of a chronic colitis with an increased interindividual variability.

To assess the effect of DSS-induced colitis on macro- and microscopic inflammatory parameters of the colon, a group of mice was sacrificed after each cycle of DSS administration (DSS cycle 1, DSS cycle 2 and DSS cycle 3, respectively, Supplementary Figure S2A). The colonic weight/length ratio was increased in all three groups (cycles 1, 2 and 3) compared to the control group (Supplementary Figure S2F). The macroscopic inflammation score was increased in all DSS cycles (Supplementary Figure S2G) with hyperemia and ulcerations abundantly present after DSS cycle 1, whereas colon thickening appeared after DSS cycles 2 and 3. Microscopic inflammation was present in all DSS groups as scored on H&E-stained colon sections (Supplementary Figure S2H) and showed crypt loss, epithelial erosions and marked infiltration of neutrophils in the colon of acute DSS treated mice (Supplementary Figure S2J). At the end of DSS cycles 2 and 3, the colon sections showed epithelial regeneration compared to the acute stage, yet with remarkable hyperplasia. Infiltration of neutrophils and lymphocytes in the submucosa and mucosa could also be observed (Supplementary Figure S2J). In addition, some mice even showed massive focal ulcerations in the colon. At the molecular level, MPO activity was increased during DSS-induced colitis progression (Supplementary Figure S2I), which confirmed the infiltration of neutrophils into the colon due to DSS administration. Interestingly, mice treated with 3 DSS cycles showed a significant lower colonic MPO activity compared to mice treated only once.

Accepted Manuscript

Downloaded from https://academic.oup.com/ecco-jcc/advance-article-abstract/doi/10.1093/ecco-jcc/jjaa015/5718468 by Universiteit Antwerpen user on 11 February 2020

3.2. Colonic inflammatory markers

In both models, colonic protein levels of several inflammatory markers were quantified (Supplementary Figure S3). At all time points post-transfer and after each cycle of DSS administration, expression of IL-1β and TNF-α was increased whereas IL-10 was reduced in expression (Supplementary Figure S3A-B, D, F-G, I). Interestingly, IL-22 protein levels were only increased at 1 and 6 weeks post-transfer and at the end of DSS cycles 1 and 3 (Supplementary Figure S3E, J). In contrast, expression of IL-6 was only increased in the more chronic phase of colitis, i.e. at week 6 post-transfer (Supplementary Figure S3C) and after the second cycle of DSS administration (Supplementary Figure S3H).

3.3. Mucosal barrier function during colitis progression

As loss of intestinal barrier integrity is recognized as a major hallmark of the IBD pathophysiology[38], changes in barrier permeability during colitis progression were investigated in both models. Results of the FITC-dextran intestinal permeability assays showed that integrity of the intestinal mucosal barrier was affected in both models (Figure 2). More specifically, FITC-dextran intestinal permeability progressively increased during colitis progression in the T cell transfer model levelling off at week 6, but remaining increased as compared to control mice (Figure 2A). In the DSS model, FITC-dextran intestinal permeability showed a strong increase after the first cycle of DSS administration, after which it declined in the chronic stages of colitis with only a significant increase left after the second DSS cycle but not after the third cycle (Figure 2B).

To further substantiate intestinal mucosal barrier dysfunction upon colitis, the expression of several components that are the building stones of and regulate the mucosal barrier were measured.

We first investigated mucin expression since they constitute the main part of the mucus layer and are the first barrier luminal pathogens and toxins encounter. *Muc2* (i.e. the main secreted mucin of

Accepted Manuscript

Downloaded from https://academic.oup.com/ecco-jcc/advance-article-abstract/doi/10.1093/ecco-jcc/jjaa015/5718468 by Universiteit Antwerpen user on 11 February 2020

the large intestine) mRNA expression was increased after 1 week post-transfer (Figure 3A) whereas it was upregulated during the chronic stages of DSS-induced colitis (Figure 4A). mRNA expression of *Muc1*, a transmembrane mucin expressed only at low levels in the healthy intestines, was upregulated after 2, 4 and 6 weeks post-transfer (Figure 3B) and after all cycles of DSS administration (Figure 4B). The transmembrane *Muc13* mucin, which is normally expressed in the healthy intestines, showed aberrant expression patterns at the RNA level in both models with an increased expression seen at 1 and 2 weeks after T cell transfer and DSS cycle 2 (Figures 3E & 4E). In contrast, mRNA expression of *Muc4*, another membrane-bound mucin, was not significantly altered during experimental colitis in either model (Figures 3D & 4D). The changes in mucin mRNA expression were verified at protein level by Western Blot and immunohistochemical stainings (Figures 3C, F, G & 4C, F, G; Supplementary Figures S4 & S5). In the DSS model, we visually observed increased Muc2 staining intensity during colitis progression, whereas in the T cell transfer model, overall Muc2 staining was not altered compared to control animals (Figures 3G & 4G). Furthermore, although Muc1 was mainly observed on the apical side of surface epithelial cells in control animals, colitis induction was associated with de novo Muc1 levels in the cytoplasm and the crypts in both colitis models (Figures 3G & 4G; Supplementary Figures S4 & S5). Muc13 staining was mainly abundant after the first two cycles of DSS administration and from week 1 post-transfer in the T cell transfer model. Concerning its subcellular localisation, Muc13 showed a strong apical expression in intestinal epithelial cells of controls, which became apparent in the cytoplasm during colitis (Figures 3G & 4G). Quantification of MUC1 and MUC13 expression by Western Blotting and IHC, confirmed the increased expression of MUC1 and MUC13 during T cell transfer and DSS-induced colitis (Figure 3C, 3F, 4C & 4F). For Muc4, no clear changes were observed during colitis progression compared to control animals (Supplementary Figures S4 & S5).

In addition, we validated the observed mucin mRNA expression patterns in colonic tissue biopsies collected from human IBD patients with active disease and in remission (Figure 5), as well as in IECs during cytokine stimulation *in vitro* (Figure 8). In line with the *in vivo* results, *MUC1* and *MUC13*

Accepted Manuscript

Downloaded from https://academic.oup.com/ecco-jcc/advance-article-abstract/doi/10.1093/ecco-jcc/jjaa015/5718468 by Universiteit Antwerpen user on 11 February 2020

expression was found to be increased in inflamed colonic biopsies compared to the adjacent non-inflamed tissue within IBD patients with active disease (Figure 5B & 5D). Treatment of LS513 cells with either TNF-α or IL-1β also significantly increased the expression of *MUC1* and *MUC13* (Figure 8). No significant differences were observed for *MUC2* ($p = 0.0781$) and *MUC4* ($p = 0.9375$) expression (Figure 5A & 5C). Furthermore, *MUC1* and *MUC2* expression was strongly upregulated in the inflamed colonic tissue from patients with active IBD compared to the non-inflamed tissue from patients in remission, whereas no differences in expression were found for *MUC13* and *MUC4* mRNA (Figure 5E-H). Overall, colonic expression of mucins did not differ between CD and UC patients in a specific condition (inflamed, non-inflamed, active or remission) (Figure 5).

Subsequently, several interesting alterations were observed in both models as far as the expression patterns of junction constituents at RNA level were concerned (Figures 6 & 7). mRNA expression levels of *Zo1* (*Tjp1*), *Tjp2*, *Jam2*, *Jam3* and Myosin Light Chain Kinase (*Mylk*) were significantly increased at week 1 post-transfer and after the first cycle of DSS administration (Figures 6A & 7A). E-cadherin (*Cdh1*) and *Ocln* mRNA expression levels were significantly decreased during the more chronic stages of experimental colitis in both models (Figures 6A & 7A) . mRNA levels of *Cldn1*, a major regulator of paracellular permeability, were elevated after the first DSS cycle, whereas it decreased throughout colitis progression in the T cell transfer model (Figures 6A & 7A) . In contrast, *Cldn2* mRNA expression was increased at 1 week post-transfer, yet its expression declined at the end of each DSS cycle (Figures 6A & 7A). In addition, *Cldn5* and *Cldn7* showed a model-specific response. More specifically, expression of *Cldn7* and *Cldn5* mRNA was upregulated at the initial stage of colitis in the T cell transfer and the DSS model, respectively (Figures 6A & 7A). Furthermore, *Tjp3* mRNA expression was reduced throughout colitis progression in the DSS-induced colitis model only, whereas *Cldn15* mRNA expression was significantly decreased during the acute phase of DSS-induced colitis and became significantly increased in the chronic phases (Figure 7A). Expression of *Cldn3* and *Jam1* was not altered throughout colitis progression in either model (Figures 6A & 7A). Immunohistochemical stainings for ZO-1 and CLDN1 were also performed to analyse alterations in

Accepted Manuscript

Downloaded from https://academic.oup.com/ecco-jcc/advance-article-abstract/doi/10.1093/ecco-jcc/jjaa015/5718468 by Universiteit Antwerpen user on 11 February 2020

intercellular junctions at the protein level. Slightly altered CLDN1 staining patterns were seen during the course of colitis in both models whereas no clear changes at protein level could visually be observed for ZO-1 (Figures 6B & 7B). To further confirm that the altered expression levels of intercellular junctions resulted from specific changes in intestinal epithelial cells, mRNA expression of several junctional proteins was studied in confluent monolayers of human IECs treated with either TNF-α or IL-1β (Figure 8). *CLDN1* and *TJP1* mRNA expression was elevated after TNF-α or IL-1β treatment, whereas *OCLN* mRNA was downregulated upon TNF-α treatment. No differences in *CDH1* mRNA expression were observed.

In addition to appropriate expression of intercellular junctions, a well organised apical-to-basal cell polarity is indispensable for the formation of a functional and tight intestinal epithelial cell monolayer[14,39,40]. Gene expression analysis showed that subunits of the different polarity complexes were affected in both our experimental colitis mouse models (Figures 9 & 10). The expression of *Par3* and *aPkcλ*, two major coordinators of tight junction localization, was downregulated at all DSS cycles and time points post-transfer (Figures 9A & 10A). On the other hand, *aPkcς* mRNA expression was only decreased in the T cell transfer model, whereas *Par6* mRNA expression was only elevated at the acute phase of DSS-induced colitis (Figures 9A & 10A). Regarding the subunits of the Crumbs polarity complex (Figures 9B & 10B), *Patj* mRNA expression tended to be decreased at all DSS cycles, whereas its expression was upregulated at week 1 post-transfer. Also mRNA expression of *Pals1* (*Mpp5*) was upregulated at the first time point of the T cell transfer model. No significant alterations in *Crb3* expression were observed in either colitis models. Interestingly, *Scrib* mRNA expression, which is known to be a negative regulator of the PAR complex[15], was increased at 1 week post-transfer and after the first DSS cycle (Figures 9C & 10C). Although evaluation of SCRIB expression in the mouse colon by immunohistochemistry did not reveal remarkable alterations in expression levels, SCRIB was found to be abundantly expressed in the goblet cells (Figures 9D & 10D). Whereas expression of *Dlg1* and *Llgl1* was altered in the T cell transfer model at 1 and 2 weeks post-transfer,

Accepted Manuscript

Downloaded from https://academic.oup.com/ecco-jcc/advance-article-abstract/doi/10.1093/ecco-jcc/jjaa015/5718468 by Universiteit Antwerpen user on 11 February 2020

respectively, no changes in expression of these subunits were observed in the DSS-colitis model (Figures 9C & 10C).

The above results highlight that epithelial cell polarity is disturbed as a consequence of colitis induction, both in the acute and chronic stages.

3.4. Aberrant mucin expression associated with loss of barrier integrity upon inflammation

It has been suggested that overexpression of transmembrane mucins in many cancer types can contribute to loss of epithelial barrier integrity by mediating junctional and cell polarity dysfunction[6,41–43]. To elucidate the involvement of aberrantly expressed transmembrane mucins as potential mediators in intestinal mucosal barrier disruption upon inflammation-induced colitis, the mucin mRNA expression data were used to perform a discriminant analysis on both models and to correlate the changes in intestinal permeability and colonic inflammation (Figures 11 & 12).

In the T cell transfer model, *Muc1* and *Muc13* expression were the best factors to discriminate whether mice developed colitis by the adoptive transfer of T cells or were controls (Figure 11A). In the DSS colitis model, *Muc2* expression was found to be the major determinant for identifying mice receiving a DSS treatment, followed by expression of *Muc1* and *Muc13* (Figure 11B). Interestingly, increased *Muc1* expression correlated significantly with increased intestinal permeability (based on FITC dextran levels in sera) in the T cell transfer model (Figure 12), whereas a positive significant correlation between aberrant *Muc13* expression and increased intestinal permeability was seen in the DSS model (Figure 14B). Furthermore, whereas IL-1β was associated with increased permeability and aberrant *Muc1* expression in T cell transfer colitis (Figure 12A & C), TNF-α positively correlated with intestinal permeability and increased *Muc13* expression in DSS-induced colitis (Figure 12B & D). Besides, the expression levels of *Muc13* also correlated with *Muc1* ($p = 0.013$) and *Muc2* ($p = 0.026$) expression in the DSS model (data not shown).

Accepted Manuscript

Downloaded from https://academic.oup.com/ecco-jcc/advance-article-abstract/doi/10.1093/ecco-jcc/jjaa015/5718468 by Universiteit Antwerpen user on 11 February 2020

In both models, altered expression of several junctional and polarity proteins correlated significantly with each other (data not shown), further indicating mutual dependence and their involvement in regulating barrier integrity. Moreover, their expression levels could also be used to discriminate between colitis mice and controls (Supplementary figure S6). Furthermore, significant associations between aberrant *Muc1*, *Cldn1*, *Ocln*, *Par3 and aPKCζ* expression in the T cell transfer model (Figure 12E&G) and between aberrant *Muc13, Cldn1*, *Jam2*, *Tjp2*, *aPkcζ*, *Crb3* and *Scrib* expression in the DSS model (Figure 12F & H) further suggested a potential role for Muc1 and Muc13 in intestinal mucosal barrier dysfunction.

4. Discussion

The intestinal mucosal barrier plays a critical role in gut health and function[5,44,45]. Not only is it a physical barrier between the microbiome, toxins and food antigens in the lumen and the internal host tissues, it also is a dynamic barrier that regulates inflammatory responses. Loss of barrier integrity is generally accepted as a major hallmark in the pathophysiology of IBD[4]. However, whether intestinal barrier dysfunction is a primary contributor to or rather a consequence of intestinal inflammation has not yet been fully elucidated[46,47]. In this study, we investigated intestinal barrier integrity and inflammation during the course of colitis using the T cell transfer and DSS mouse models. In addition, mucin expression was validated in colon biopsies from IBD patients. In both models, increased permeability in association with an innate inflammatory response, as characterized by increased expression of the pro-inflammatory cytokines TNF-α and IL-1β and decreased expression of the anti-inflammatory cytokine IL-10, was already seen at 1 week post-transfer and after the first DSS administration, and was maintained during the course of disease. Excessive production of TNF-α and IL-1β has been described in IBD patients and these harmful cytokines, produced by T cells, macrophages and neutrophils, are likely to affect intestinal homeostasis leading to further aggravation of inflammation[48–50]. In our study, increased expression of IL-6 appeared only in later stages of colitis progression. This pro-inflammatory cytokine has been shown to be an important mediator of Th17 cell differentiation, further promoting intestinal

Accepted Manuscript

Downloaded from https://academic.oup.com/ecco-jcc/advance-article-abstract/doi/10.1093/ecco-jcc/jjaa015/5718468 by Universiteit Antwerpen user on 11 February 2020

inflammation in IBD and modulating intestinal epithelial cells[51,52]. Also IL-22 was increasingly expressed at the beginning of colitis induction and even at week 6 post-transfer and after the last DSS cycle. This cytokine is normally able to promote mucosal healing in the intestine, but when uncontrolled, it can lead to intestinal inflammation[53,54]. Based on the above findings, we cannot clearly substantiate whether loss of barrier integrity could be a primary defect. However, expression analysis of junctional proteins and polarity complexes in both our models revealed that most changes already occurred at the beginning of colitis development. This would suggest that loss of barrier integrity is not only a result of an innate inflammatory response but might also be a primary contributor in the pathophysiology of IBD.

The key mediators underlying mucosal barrier dysfunction upon inflammation in IBD still remain to be further elucidated. Often overlooked in intestinal barrier research are the mucins. These heavily glycosylated proteins make up the first part of the barrier, the mucus layer, which is four times thicker than the actual epithelial cell layer and plays an important role in limiting contact between the host and the luminal content[55]. MUC2 is the main component of the secreted mucus layer and provides the first line of defence against invading pathogens and toxins in the intestines. In IBD, this secretory mucin is critical for colonic protection since it has been shown that *Muc2*$^{-/-}$ mice spontaneously develop colitis[24]. The gradual increase in Muc2 expression seen during the course of colitis in the DSS model can thus be assigned to the host defence to overcome the toxic effects of DSS on the colonic epithelium. Furthermore, although several studies have shown a downregulation of this mucin in the intestinal mucosae of IBD patients[56–58], we could not confirm this in our own IBD patient cohort.

Since transmembrane mucins are increasingly expressed in IBD[26,38,56] and given their role in signalling pathways involved in cell-cell adhesion and cell differentiation, they are excellent candidates to be involved in the regulation of the barrier function[6,59] In our study, expression of the transmembrane Muc1 and Muc13 mucins was increased during colitis progression in both models, as well as during

Accepted Manuscript

Downloaded from https://academic.oup.com/ecco-jcc/advance-article-abstract/doi/10.1093/ecco-jcc/jjaa015/5718468 by Universiteit Antwerpen user on 11 February 2020

cytokine stimulation in IECs and in inflamed colonic tissue of active IBD patients. Furthermore, MUC1 expression was also increased in our patient cohort with active disease compared to patients in remission, whereas such differences in expression were not seen for MUC13. A possible explanation for this latter finding might be that a subset of IBD patients in clinical remission still have subclinical inflammation and intestinal barrier dysfunction. On the other hand, Muc4 showed variable expression patterns in the inflamed murine colon. Variable MUC4 expression has also been reported in IBD patients as validated by our own human data and increased MUC4 expression was mainly observed in UC patients with neoplastic conditions[60]. Inappropriate overexpression of transmembrane mucins, such as MUC1 and MUC13 induced by pro-inflammatory cytokines, could lead to aberrant modulation of mucosal epithelial cell inflammatory signalling, which in turn could lead to pathological inflammation[38,61]. Furthermore, acute DSS studies with knockout animals showed that *Muc1*$^{-/-}$ mice were resistant to inflammation-induced colitis whereas *Muc13*$^{-/-}$ mice developed more inflammation compared to wildtype animals[26,62]. In our DSS model, Muc13 expression was altered in both the acute and chronic phases of DSS-induced colitis. This increase in expression in the more chronic stage of colitis was also confirmed in the T cell transfer model. Unlike MUC1, MUC13 is highly expressed by the intestinal epithelium playing at first a protective role against cytotoxic agents[26,63]. Furthermore, Sheng and colleagues[29] demonstrated that MUC13 has a pro-inflammatory activity in the intestinal epithelium modulating inflammatory responses induced by TNF-α. Also in our DSS models, increased TNF-α expression was significantly associated with altered *Muc13* expression, further suggesting that expression of this mucin is regulated by TNF-α upon inflammation and thus, the role of this mucin upon chronic colitis should be further investigated. In addition, we were able to correctly annotate individual mice to their experimental group (i.e. control or different time points of colitis) based on *Muc1* and *Muc13* expression (Figure 11). Interestingly, three main clusters could be distinguished in both colitis models. In particular, mice that were sacrificed during the initial stages of colitis (after 1 cycle of DSS administration and after 1 week of T cell transfer) were separated from both the control mice and the other

Accepted Manuscript

Downloaded from https://academic.oup.com/ecco-jcc/advance-article-abstract/doi/10.1093/ecco-jcc/jjaa015/5718468 by Universiteit Antwerpen user on 11 February 2020

experimental groups. Mice that were sacrificed at later time points could clearly be distinguished from control mice yet were more closely associated. These results further indicate the importance of Muc1 and Muc13 during the course of colitis.

To the best of our knowledge, a clear association between increased expression of transmembrane mucins and barrier dysfunction in IBD, has so far never been reported. Here, we found a positive correlation between increased *Muc1* and *Muc13* expression and increased *in vivo* intestinal barrier permeability to 4 kDa FITC-dextran during colitis progression, which was further substantiated by a strong correlation between expression of these mucins and altered expression of barrier mediators, including junctional and polarity proteins. Also observed was a model-specific response for both mucins, which could be explained by the different mechanisms of colitis induction. Whereas colitis in the T cell transfer model is induced by disrupting systemic T cell homeostasis, DSS is toxic to the intestinal epithelium leading to the penetration of luminal bacteria and antigens through the intestinal barrier resulting in a strong innate inflammatory response[64]. Since MUC13 is highly expressed at the healthy intestinal epithelium, its role in modulating the integrity of the intestinal barrier could be related to immediate threats from the external environment. MUC1, on the other hand, is expressed at low levels in the healthy intestine and thus its involvement in barrier dysfunction could be dependent on the infiltration of T lymphocytes upon an inflammatory stimulus. Although similar cytokine profiles were associated with disease activity in both models, IL-1β was correlated to increased *Muc1* expression and *in vivo* FITC-dextran intestinal permeability in the T cell transfer model and TNF-α to increased *Muc13* expression and *in vivo* FITC-dextran intestinal permeability in the DSS-induced colitis model. Furthermore, MUC1 and MUC13 were also shown to be upregulated in confluent IEC monolayers by the stimulation with either TNF-α or IL-1β in vitro. Whereas TNF-α exerted the strongest effects on both mucins, IL-1β also induced a significant increase in MUC13 expression and a trend towards a significant elevation of MUC1 expression. Hence, subtle differences in cytokine secretion could induce specific changes in mucin expression in both models. Nevertheless, based on the above findings, we can conclude that aberrantly expressed

Accepted Manuscript

Downloaded from https://academic.oup.com/ecco-jcc/advance-article-abstract/doi/10.1093/ecco-jcc/jjaa015/5718468 by Universiteit Antwerpen user on 11 February 2020

Muc1 and Muc13 could play a role in modulating intestinal barrier dysfunction during the course of colitis.

Overexpression of transmembrane mucins can result in a repositioning over the whole cell membrane, causing physical hindrance of neighbouring cells to make cell contact[6]. In our control animals, Muc1 and Muc13 were expressed at the apical side of the epithelial membrane, whereas they became generally visible throughout the cell during colitis progression. Transmembrane mucins can affect cell-cell interactions, and thus barrier functionality, in multiple ways. First, via extracellular EGF-like domains and intracellular phosphorylation sites, they can interact with receptor tyrosine kinases, such as ERBB2[7]. Activation of this membrane-bound receptor can then result in a disruption of the PAR polarity complex and subsequent tight junction dysfunction by associating with Par6 and aPKC and blocking the interaction with Par3[65]. The mRNA expression of PAR3 and aPKC-lambda was shown to be decreased during the course of colitis in both mouse models. This indicates an overall disturbance of the PAR-complex during both acute and recurrent, chronic colitis. Nevertheless, future research should certainly focus on elucidating the role of the individual subunits in intestinal barrier dysfunction in IBD. Furthermore, a correlation between increased *Muc1* expression and decreased *Par3* expression was found suggesting that loss of barrier integrity mediated by Muc1 might be caused by sequestering with ERBB2 and subsequent dissociation of the PAR complex. Interaction of MUC1, but also MUC4 and MUC13, with ERBB2 has been described in many cancer types[66–68] and the role of ERBB2 in barrier functionality in IBD remains to be further investigated. Second, the cytoplasmic domain of transmembrane mucins can be transported into the nucleus and suppress transcription of crumbs and scribble polarity genes, via interaction with a transcription factor on the promoter of these polarity genes[13]. In this way, loss of cell polarity and tight junction dysfunction can be induced as well. Here, we found a correlation between the expression levels of *Muc13*, *Crb3 and Scrib* in the DSS model, highlighting that these mucins could probably also act according to the mechanism described above. Additionally, it has also been described that MUC1 can intracellularly interact with β-catenin, which results in the disruption of the E-cadherin/β-catenin

Accepted Manuscript

Downloaded from https://academic.oup.com/ecco-jcc/advance-article-abstract/doi/10.1093/ecco-jcc/jjaa015/5718468 by Universiteit Antwerpen user on 11 February 2020

complex and eventually leads to loss of adherens junction stability[69]. In our colitis models, however, increased *Muc1* and *Muc13* expression was not associated with altered *Cdh1* (E-cadherin) expression.

Taken together, the results from our study clearly show the association of aberrant Muc1 and Muc13 expression with intestinal mucosal barrier dysfunction during the course of colitis. A model-specific response was observed, indicating a complex transcriptional regulation of mucin expression that results from the combined effects of the host inflammatory response, the microbiome and the type and course of disease. Nevertheless, the exact mechanisms by which these mucins affect barrier integrity and to prove their functional role in barrier integrity in IBD require further investigation.

Most available therapies in IBD are directed against the inflammatory response. Due to the clinical heterogeneity of these diseases, biologicals are limited in efficacy and safety and still a substantial number of patients fail to respond or obtain full remission[3]. Targeting the barrier, and particularly MUC1 and MUC13, could also have therapeutic potential. These transmembrane mucins have already shown their potential in antibody-based therapy in different cancer types, including colon cancer, making them valuable therapeutic targets in medicine[6,70]. Furthermore, mucins are highly polymorphic and gene polymorphisms affecting mucin expression have been reported to influence susceptibility towards disease[56]. The presence of genetic differences in mucin genes can result in different mRNA isoforms (i.e. splice variants via alternative splicing) produced from the same mucin gene locus. While most isoforms encode similar biological functions, others have the potential to alter the protein function resulting in progression toward disease[56]. So far, only the MUC13-R502S polymorphism has been related to UC and the MUC1-rs3180018 to CD but the MUC1 and MUC13 isoforms associated with IBD remain unknown as well. Inhibiting inflammation-induced MUC1 and MUC13 isoforms to restore intestinal barrier integrity may thus achieve greater efficacy with fewer side effects.

Accepted Manuscript

Downloaded from https://academic.oup.com/ecco-jcc/advance-article-abstract/doi/10.1093/ecco-jcc/jjaa015/5718468 by Universiteit Antwerpen user on 11 February 2020

Manuscript Doi: 10.1093/ecco-jcc/jjaa015

Overall, it is highlighted here that aberrantly expressed Muc1 and Muc13 might be involved in intestinal mucosal barrier dysfunction upon inflammation by affecting tight junction and cell polarity proteins and that they can act as possible targets for novel therapeutic interventions.

Accepted Manuscript

Funding

This work was supported by the University of Antwerp [DOCPRO4 34782, TOP-BOF 35018]. The Leica SP 8 microscope was funded by the Hercules Foundation of the Flemish Government [Hercules grant AUHA.15.12].

Downloaded from https://academic.oup.com/ecco-jcc/advance-article-abstract/doi/10.1093/ecco-jcc/jjaa015/5718468 by Universiteit Antwerpen user on 11 February 2020

Manuscript Doi: 10.1093/ecco-jcc/jjaa015

Conflict of Interest

The authors have no competing interests.

Author contributions

TB, HVS, AS, JDM, and BDW contributed to the concept and design of the study. TB (DSS model) and HVS (T cell transfer model) performed the fundamental experiments. AJA, EM, HDS and TB were responsible for patient inclusion and collection of colonic tissue samples from IBD patients. TB, HVS and AS wrote the manuscript. All the authors contributed to the analysis and interpretation of data and critically reviewed and approved the final draft.

Acknowledgements

We thank Petra Aerts, Neslihan Bas, Jacky de Leeuw, Angelika Jürgens, Ilse Goolaerts, Rita Van Den Bossche, Marleen Vinckx, Lieve Vits and Dominique De Rijck for their skilled technical assistance.

Accepted Manuscript

Downloaded from https://academic.oup.com/ecco-jcc/advance-article-abstract/doi/10.1093/ecco-jcc/jjaa015/5718468 by Universiteit Antwerpen user on 11 February 2020

Manuscript Doi: 10.1093/ecco-jcc/jjaa015

References

1. Podolsky DK. Inflammatory Bowel Disease. *N Engl J Med* 2002; 347(6): 417–29.

2. Shen B. IBD: Step-up vs top-down therapy for Crohn's disease: medicine vs surgery. *Nat Rev Gastroenterol Hepatol* 2017; 14(12): 693–5.

3. Jauregui-Amezaga A, Somers M, De Schepper H, Macken E. Next generation of biologics for the treatment of Crohn's disease: an evidence-based review on ustekinumab. *Clin Exp Gastroenterol* 2017; 10: 293–301.

4. McGuckin MA, Eri R, Simms LA, et al. Intestinal barrier dysfunction in inflammatory bowel diseases. *Inflamm Bowel Dis* 2009; 15(1): 100–13.

5. Odenwald MA, Turner JR. The intestinal epithelial barrier: a therapeutic target? *Nat Rev Gastroenterol Hepatol* 2017; 14(1): 9–21.

6. Kufe DW. Mucins in cancer: function, prognosis and therapy. *Nat Rev Cancer* 2009; 9(12): 874–85.

7. van Putten JPM, Strijbis K. Transmembrane Mucins: Signaling Receptors at the Intersection of Inflammation and Cancer. *J Innate Immun* 2017; 9(3): 281–99.

8. Peterson LW, Artis D. Intestinal epithelial cells: regulators of barrier function and immune homeostasis. *Nat Rev Immunol* 2014; 14(3): 141–53.

9. van der Flier LG, Clevers H. Stem Cells, Self-Renewal, and Differentiation in the Intestinal Epithelium. *Annu Rev Physiol* 2009; 71(1): 241–60.

10. Luissint A-C, Parkos CA, Nusrat A. Inflammation and the Intestinal Barrier: Leukocyte-

Accepted Manuscript

Downloaded from https://academic.oup.com/ecco-jcc/advance-article-abstract/doi/10.1093/ecco-jcc/jjaa015/5718468 by Universiteit Antwerpen user on 11 February 2020

Epithelial Cell Interactions, Cell Junction Remodeling, and Mucosal Repair. *Gastroenterology* 2016; 151(4): 616–32.

11. Liang GH, Weber CR. Molecular aspects of tight junction barrier function. *Curr Opin Pharmacol* 2014; 19: 84–9.

12. Yamanaka T, Horikoshi Y, Suzuki A, et al. PAR-6 regulates aPKC activity in a novel way and mediates cell-cell contact-induced formation of the epithelial junctional complex. *Genes to Cells* 2001; 6(8): 721–31.

13. Alam M, Bouillez A, Tagde A, et al. MUC1-C Represses the Crumbs Complex Polarity Factor CRB3 and Downregulates the Hippo Pathway. *Mol Cancer Res* 2016; 14(12): 1266–76.

14. Whiteman EL, Fan S, Harder JL, et al. Crumbs3 is essential for proper epithelial development and viability. *Mol Cell Biol* 2014; 34(1): 43–56.

15. Yamanaka T, Ohno S. Role of Lgl/Dlg/Scribble in the regulation of epithelial junction, polarity and growth. *Front Biosci* 2008; 13: 6693–707.

16. Li B, Alli R, Vogel P, Geiger TL. IL-10 modulates DSS-induced colitis through a macrophage-ROS-NO axis. *Mucosal Immunol* 2014; 7(4): 869–78.

17. Li Y, Adam R, Colombel J-F, Bian Z. A characterization of pro-inflammatory cytokines in dextran sulfate sodium-induced chronic relapsing colitis mice model. *Int Immunopharmacol* 2018; 60: 194–201.

18. De Fazio L, Cavazza E, Spisni E, et al. Longitudinal analysis of inflammation and microbiota dynamics in a model of mild chronic dextran sulfate sodium-induced colitis in mice. *World J Gastroenterol* 2014; 20(8): 2051–61.

19. Wang Y, Lin F, Zhu X, et al. Distinct roles of intracellular heat shock protein 70 in maintaining gastrointestinal homeostasis. *Am J Physiol Gastrointest Liver Physiol* 2018; 314(2): G164–78.

Accepted Manuscript

Downloaded from https://academic.oup.com/ecco-jcc/advance-article-abstract/doi/10.1093/ecco-jcc/jjaa015/5718468 by Universiteit Antwerpen user on 11 February 2020

20. Laukoetter MG, Nava P, Lee WY, et al. JAM-A regulates permeability and inflammation in the intestine in vivo. *J Exp Med* 2007; 204(13): 3067–76.

21. Han F, Zhang H, Xia X, et al. Porcine β-defensin 2 attenuates inflammation and mucosal lesions in dextran sodium sulfate-induced colitis. *J Immunol* 2015; 194(4): 1882–93.

22. Luettig J, Rosenthal R, Barmeyer C, Schulzke JD. Claudin-2 as a mediator of leaky gut barrier during intestinal inflammation. *Tissue Barriers* 2015; 3(1): e977176.

23. Eichele DD, Kharbanda KK. Dextran sodium sulfate colitis murine model: An indispensable tool for advancing our understanding of inflammatory bowel diseases pathogenesis. *World J Gastroenterol* 2017; 23(33): 6016–29.

24. Van der Sluis M, De Koning BAE, De Bruijn ACJM, et al. Muc2-Deficient Mice Spontaneously Develop Colitis, Indicating That MUC2 Is Critical for Colonic Protection. *Gastroenterology* 2006; 131(1): 117–29.

25. Petersson J, Schreiber O, Hansson GC, et al. Importance and regulation of the colonic mucus barrier in a mouse model of colitis. *Am J Physiol Gastrointest Liver Physiol* 2011; 300(2): G327-33.

26. Sheng YH, Lourie R, Lindén SK, et al. The MUC13 cell-surface mucin protects against intestinal inflammation by inhibiting epithelial cell apoptosis. *Gut* 2011; 60(12): 1661–70.

27. Banerjee D, Fernandez HR, Patil PB, et al. Epithelial MUC1 promotes cell migration, reduces apoptosis and affects levels of mucosal modulators during acetylsalicylic acid (aspirin)-induced gastropathy. *Biochem J* 2015; 465(3): 423–31.

28. Vermeer PD, Einwalter LA, Moninger TO, et al. Segregation of receptor and ligand regulates activation of epithelial growth factor receptor. *Nature* 2003; 422(6929): 322–6.

29. Sheng Y, Triyana S, Wang R, et al. MUC1 and MUC13 differentially regulate epithelial

Accepted Manuscript

Downloaded from https://academic.oup.com/ecco-jcc/advance-article-abstract/doi/10.1093/ecco-jcc/jjaa015/5718468 by Universiteit Antwerpen user on 11 February 2020

inflammation in response to inflammatory and infectious stimuli. *Mucosal Immunol* 2012; 6(3): 557–68.

30. Kiesler P, Fuss IJ, Strober W. Experimental Models of Inflammatory Bowel Diseases. *Cell Mol Gastroenterol Hepatol* 2015; 1(2): 154–70.

31. Mashukova A, Wald FA, Salas PJ. Tumor necrosis factor alpha and inflammation disrupt the polarity complex in intestinal epithelial cells by a posttranslational mechanism. *Mol Cell Biol* 2011; 31(4): 756–65.

32. Heylen M, Ruyssers NE, De Man JG, et al. Worm proteins of Schistosoma mansoni reduce the severity of experimental chronic colitis in mice by suppressing colonic proinflammatory immune responses. *PLoS One* 2014; 9(10): e110002.

33. Heylen M, Deleye S, De Man JG, et al. Colonoscopy and µPET/CT are Valid Techniques to Monitor Inflammation in the Adoptive Transfer Colitis Model in Mice. *Inflamm Bowel Dis* 2013; 19(5): 967–76.

34. Wallace JL, Keenan CM, Gale D, Shoupe TS. Exacerbation of experimental colitis by nonsteroidal anti-inflammatory drugs is not related to elevated leukotriene B4synthesis. *Gastroenterology* 1992; 102(1): 18–27.

35. Moreels TG, Nieuwendijk RJ, De Man JG, et al. Concurrent infection with Schistosoma mansoni attenuates inflammation induced changes in colonic morphology, cytokine levels, and smooth muscle contractility of trinitrobenzene sulphonic acid induced colitis in rats. *Gut* 2004; 53(1): 99–107.

36. Ruyssers NE, De Winter BY, De Man JG, et al. Therapeutic potential of helminth soluble proteins in TNBS-induced colitis in mice. *Inflamm Bowel Dis* 2009; 15(4): 491–500.

37. Gupta J, Nebreda A. Analysis of Intestinal Permeability in Mice. *BIO-PROTOCOL* 2014; 4(22).

Accepted Manuscript

Downloaded from https://academic.oup.com/ecco-jcc/advance-article-abstract/doi/10.1093/ecco-jcc/jjaa015/5718468 by Universiteit Antwerpen user on 11 February 2020

38. Vancamelbeke M, Vanuytsel T, Farré R, et al. Genetic and Transcriptomic Bases of Intestinal Epithelial Barrier Dysfunction in Inflammatory Bowel Disease. *Inflamm Bowel Dis* 2017; 23(10): 1718–29.

39. Ivanov AI, Young C, Den Beste K, et al. Tumor suppressor scribble regulates assembly of tight junctions in the intestinal epithelium. *Am J Pathol* 2010; 176(1): 134–45.

40. Schumann M, Günzel D, Buergel N, et al. Cell polarity-determining proteins Par-3 and PP-1 are involved in epithelial tight junction defects in coeliac disease. *Gut* 2012; 61(2): 220–8.

41. Mukhopadhyay P, Lakshmanan I, Ponnusamy MP, et al. MUC4 overexpression augments cell migration and metastasis through EGFR family proteins in triple negative breast cancer cells. *PLoS One* 2013; 8(2): e54455.

42. Khan S, Sikander M, Ebeling MC, et al. MUC13 interaction with receptor tyrosine kinase HER2 drives pancreatic ductal adenocarcinoma progression. *Oncogene* 2017; 36(4): 491–500.

43. Fernandez HR, Lindén SK. The aspirin metabolite salicylate inhibits lysine acetyltransferases and MUC1 induced epithelial to mesenchymal transition. *Sci Rep* 2017; 7(1): 5626.

44. Zarepour M, Bhullar K, Montero M, et al. The mucin Muc2 limits pathogen burdens and epithelial barrier dysfunction during Salmonella enterica serovar Typhimurium colitis. *Infect Immun* 2013; 81(10): 3672–83.

45. Van Spaendonk H, Ceuleers H, Witters L, et al. Regulation of intestinal permeability: The role of proteases. *World J Gastroenterol* 2017; 23(12): 2106–23.

46. Vancamelbeke M, Vermeire S. The intestinal barrier: a fundamental role in health and disease. *Expert Rev Gastroenterol Hepatol* 2017; 11(9): 821–34.

47. Laukoetter MG, Nava P, Nusrat A. Role of the intestinal barrier in inflammatory bowel disease. *World J Gastroenterol* 2008; 14(3): 401–7.

Accepted Manuscript

Downloaded from https://academic.oup.com/ecco-jcc/advance-article-abstract/doi/10.1093/ecco-jcc/jjaa015/5718468 by Universiteit Antwerpen user on 11 February 2020

48. Tracey, M.D KJ, Cerami, Ph.D A. Tumor Necrosis Factor: A Pleiotropic Cytokine and Therapuetic Target. *Annu Rev Med* 1994; 45(1): 491–503.

49. Neurath MF. Cytokines in inflammatory bowel disease. *Nat Rev Immunol* 2014; 14(5): 329–42.

50. Martini E, Krug SM, Siegmund B, et al. Mend Your Fences: The Epithelial Barrier and its Relationship With Mucosal Immunity in Inflammatory Bowel Disease. *Cell Mol Gastroenterol Hepatol* 2017; 4(1): 33–46.

51. Zhou L, Ivanov II, Spolski R, et al. IL-6 programs TH-17 cell differentiation by promoting sequential engagement of the IL-21 and IL-23 pathways. *Nat Immunol* 2007; 8(9): 967–74.

52. Kinugasa T, Sakaguchi T, Gu X, Reinecker H. Claudins regulate the intestinal barrier in response to immune mediators. *Gastroenterology* 2000; 118(6): 1001–11.

53. Sonnenberg GF, Fouser LA, Artis D. Border patrol: regulation of immunity, inflammation and tissue homeostasis at barrier surfaces by IL-22. *Nat Immunol* 2011; 12(5): 383–90.

54. Huber S, Gagliani N, Zenewicz LA, et al. IL-22BP is regulated by the inflammasome and modulates tumorigenesis in the intestine. *Nature* 2012; 491(7423): 259–63.

55. Linden S, Putton P, Karlsson N, et al. Mucins in the mucosal barrier to infection. *Mucosal Immunol* 2008; 1(3): 183–97.

56. Moehle C, Ackermann N, Langmann T, et al. Aberrant intestinal expression and allelic variants of mucin genes associated with inflammatory bowel disease. *J Mol Med* 2006; 84(12): 1055–66.

57. Klinken BJ-W Van, Wal J-WG Van der, Einerhand A, et al. Sulphation and secretion of the predominant secretory humancolonic mucin MUC2 in ulcerative colitis. *Gut* 1999; 44(3): 387.

Accepted Manuscript

Downloaded from https://academic.oup.com/ecco-jcc/advance-article-abstract/doi/10.1093/ecco-jcc/jjaa015/5718468 by Universiteit Antwerpen user on 11 February 2020

58. Tytgat KMAJ, van der Wal J-WG, Einerhand AWC, et al. Quantitative Analysis of MUC2 Synthesis in Ulcerative Colitis. *Biochem Biophys Res Commun* 1996; 224(2): 397–405.

59. Sheng YH, Hasnain SZ, Florin THJ, McGuckin MA. Mucins in inflammatory bowel diseases and colorectal cancer. *J Gastroenterol Hepatol* 2012; 27(1): 28–38.

60. Myerscough N, Warren B, Gough M, Corfield A. Expression of mucin genes in ulcerative colitis. *Biochem Soc Trans* 1995; 23(4): 536S.

61. Sheng YH, Hasnain SZ, Florin THJ, McGuckin MA. Mucins in inflammatory bowel diseases and colorectal cancer. *J Gastroenterol Hepatol* 2012; 27(1): 28–38.

62. Das S, Rachagani S, Sheinin Y, et al. Mice deficient in Muc4 are resistant to experimental colitis and colitis-associated colorectal cancer. *Oncogene* 2016; 35(20): 2645–54.

63. Sheng YH, He Y, Hasnain SZ, et al. MUC13 protects colorectal cancer cells from death by activating the NF-κB pathway and is a potential therapeutic target. *Oncogene* 2017; 36(5): 700–13.

64. Kiesler P, Fuss IJ, Strober W. Experimental Models of Inflammatory Bowel Diseases. *Cell Mol Gastroenterol Hepatol* 2015; 1(2): 154–70.

65. Aranda V, Haire T, Nolan ME, et al. Par6–aPKC uncouples ErbB2 induced disruption of polarized epithelial organization from proliferation control. *Nat Cell Biol* 2006; 8(11): 1235–45.

66. Khan S, Sikander M, Ebeling MC, et al. MUC13 interaction with receptor tyrosine kinase HER2 drives pancreatic ductal adenocarcinoma progression. *Oncogene* 2017; 36(4): 491–500.

67. Raina D, Uchida Y, Kharbanda A, et al. Targeting the MUC1-C oncoprotein downregulates HER2 activation and abrogates trastuzumab resistance in breast cancer cells. *Oncogene* 2014; 33(26): 3422–31.

Accepted Manuscript

Downloaded from https://academic.oup.com/ecco-jcc/advance-article-abstract/doi/10.1093/ecco-jcc/jjaa015/5718468 by Universiteit Antwerpen user on 11 February 2020

68. Chaturvedi P, Singh AP, Chakraborty S, et al. MUC4 mucin interacts with and stabilizes the HER2 oncoprotein in human pancreatic cancer cells. *Cancer Res* 2008; 68(7): 2065–70.

69. Roy LD, Sahraei M, Subramani DB, et al. MUC1 enhances invasiveness of pancreatic cancer cells by inducing epithelial to mesenchymal transition. *Oncogene* 2011; 30(12): 1449–59.

70. Maher DM, Gupta BK, Nagata S, et al. Mucin 13: Structure, Function, and Potential Roles in Cancer Pathogenesis. *Mol Cancer Res* 2011; 9(5): 531–7.

Accepted Manuscript

Downloaded from https://academic.oup.com/ecco-jcc/advance-article-abstract/doi/10.1093/ecco-jcc/jjaa015/5718468 by Universiteit Antwerpen user on 11 February 2020

Manuscript Doi: 10.1093/ecco-jcc/jjaa015

Figure legends

Figure 1. **Schematic representation of the intestinal mucosal barrier.** The intestinal barrier comprises a thick layer of mucus, a single layer of epithelial cells and the inner lamina propria hosting innate and adaptive immune cells. Secreted and transmembrane mucins (MUCs) represent the major components of the mucus barrier. Besides having a protective function, transmembrane mucins also participate in intracellular signal transduction. The epithelium underneath plays an active role in innate immunity via secretion and expression of mucins and antimicrobial peptides as well as by hosting antigen presenting cells. Intestinal epithelial cells are tightly linked to each other by intercellular junctions: i.e. tight junctions (claudins (CLDNs), occludin (OCLN), tricellulin and junctional adhesion molecules (JAMs)) and adherens junctions (E-cadherin and β-catenin). The PAR, Crumbs and Scribble polarity complexes regulate the polarized expression of membrane proteins in the epithelial cells.

Figure 2. Analysis of 4 kDa FITC-dextran intestinal permeability in the T-cell transfer and DSS-induced colitis models. Relative gastrointestinal permeability of control mice compared to colitis animals: **(A)** T cell transfer model (N = 7-10 mice/group (week 0 (control), 1, 2, 4 & 6)); **(B)** DSS model (N = 8-13 mice/group (control, DSS cycle 1, DSS cycle 2, DSS cycle 3)). Significant differences between control and colitis mice are indicated by *p<0.05; **p<0.01; ***p<0.001 (Kruskal-Wallis test, Dunn's post-hoc multiple comparison test).

Figure 3. Colonic mucin expression in the adoptive T cell transfer model. (A-B, D-E) mRNA expression of *Muc1*, *Muc2*, *Muc4* and *Muc13* in the colon of controls and T cell transfer-induced

Accepted Manuscript

Downloaded from https://academic.oup.com/ecco-jcc/advance-article-abstract/doi/10.1093/ecco-jcc/jjaa015/5718468 by Universiteit Antwerpen user on 11 February 2020

colitis mice (N = 7-10 mice/group (week 0 (control), 1, 2, 4 & 6)). **(C, F)** Protein expression of Muc1 and Muc13 by quantification of the percentage of brown staining (Muc1 (C)/Muc13 (F)) in 3 randomly chosen intestinal crypts in the colon of controls and T cell transfer-induced colitis mice (N = 3 mice/group (week 0 (control), 1, 2, 4 & 6)). Significant differences between control and colitis mice are indicated by *p<0.05; **p<0.01; ***p<0.001 (One-Way ANOVA, Tukey's post-hoc multiple comparison test). **(G)** Immunohistochemistry was assessed to analyse Muc1, Muc2, Muc4 and Muc13 protein expression during the course of colitis. Representative images were selected. The scale bars are 20 µm.

Figure 4. Colonic mucin expression in the DSS-induced colitis model. (A-B, D-E) mRNA expression of *Muc1*, *Muc2*, *Muc4* and *Muc13* in the colon of controls and DSS-induced colitis mice (N = 10-13 mice/group (control, DSS cycle 1, DSS cycle 2, DSS cycle 3)). **(C, F)** Protein expression of Muc1 and Muc13 by Western blotting in the colon of controls and DSS-induced colitis mice (N = 3 mice/group (control, DSS cycle 1, DSS cycle 2, DSS cycle 3)). Significant differences between control and colitis mice are indicated by *p<0.05; **p<0.01; ***p<0.001 (One-Way ANOVA, Tukey's post-hoc multiple comparison test). **(G)** Immunohistochemistry was assessed to investigate Muc1, Muc2, Muc4 and Muc13 protein expression. Representative images were selected. The scale bars shown are 20 µm.

Figure 5. Mucin expression in colonic tissue from human IBD patients. mRNA expression of *MUC1*, *MUC2*, *MUC4* and *MUC13* in colonic biopsy tissues comparing **(A-D)** inflamed and non-inflamed colonic tissue from IBD patients with active disease (N = 7) and **(E-H)** colonic tissue from IBD patients with active disease (N = 13) and in remission (N = 15). Significant differences are indicated by *p<0.05; **p<0.01; ***p<0.001 (Wilcoxon matched-pairs signed-rank test (inflamed vs non-inflamed colonic tissue) or Mann-Whitney U test (colonic tissue from IBD patients with active disease vs IBD

Accepted Manuscript

Downloaded from https://academic.oup.com/ecco-jcc/advance-article-abstract/doi/10.1093/ecco-jcc/jjaa015/5718468 by Universiteit Antwerpen user on 11 February 2020

patients in remission)). Full circles represent patients with ulcerative colitis, open circles represent patients with Crohn's disease.

Figure 6. Colonic intercellular junction expression in the adoptive T cell transfer model. (A) mRNA expression of several Claudins (*Cldn*), Zonula-Occludens (*Zo/Tjp*), Junctional Adhesion Molecules (*Jam*), Occludin (*Ocln*), E-cadherin (*Cdh1*) and Myosin light chain kinase (*Mylk*) in the colon of controls and T cell transfer-induced colitis mice. Significant differences between healthy control and colitis mice are indicated by *p<0.05; **p<0.01; ***p<0.001 (N = 10-13 mice/group (week 0 (control), 1, 2, 4 & 6); One-Way ANOVA or Kruskal-Wallis, Tukey's and Dunn's multiple comparison post-hoc test). **(B)** Immunohistochemical analysis of ZO-1 and CLDN1. Representative confocal z-stack images of maximal intensity projections at different stages of colitis (week 0, 1 & 4) are shown. The scale bars are 25 µm.

Figure 7. Colonic intercellular junction expression in the DSS model. (A) mRNA expression of several Claudins (*Cldn*), Zonula-Occludens (*Zo/Tjp*), Junctional Adhesion Molecules (*Jam*), Occludin (*Ocln*), E-cadherin (*Cdh1*) and Myosin light chain kinase (*Mylk*) in the colon of controls and DSS-induced colitis mice. Significant differences between control and colitis mice are indicated by *p<0.05; **p<0.01; ***p<0.001 (N = 10-13 mice/group (control, DSS cycle 1, DSS cycle 2, DSS cycle 3); One-Way ANOVA or Kruskal-Wallis, Tukey's and Dunn's multiple comparison post-hoc test). **(B)** Immunohistochemical analysis of ZO-1 and CLDN1. Representative images of control mice compared to colitis mice are shown. Large panels: confocal z-stack images of maximal intensity projections (the scale bars are 25 µm). Inset panels: single plane confocal images (the scale bars are 10 µm).

Accepted Manuscript

Downloaded from https://academic.oup.com/ecco-jcc/advance-article-abstract/doi/10.1093/ecco-jcc/jjaa015/5718468 by Universiteit Antwerpen user on 11 February 2020

Figure 8. Mucin and intercellular junction expression in LS513 intestinal epithelial cells during cytokine stimulation. mRNA expression analysis of *MUC1, MUC13*, *CLDN1*, *OCLN*, *TJP1* and CDH1 expression in confluent LS513 cell monolayers after stimulation with 40 ng/ml TNF-α or IL-1β for 24 hours. Untreated cells were included as controls. Significant differences between cytokine-stimulated and untreated cells are indicated by *p<0.05; **p<0.01; ***p<0.001 (One-Way ANOVA, Tukey's post-hoc multiple comparison test, N = 3).

Figure 9. Colonic expression of cell polarity proteins during the course of adoptive T cell transfer colitis in mice. mRNA expression of **(A)** *Par3*, *Par6*, *aPkcλ* and *aPkcς* (PAR complex) **(B)** *Crb3*, *Pals1* and *Patj* (Crumbs complex) and **(C)** *Scrib*, *Dlg1* and *Llgl1* (Scribble complex) in the T cell transfer (N = 7-10 mice/group (week 0 (control), 1, 2, 4 & 6)). Significant differences between control and colitis mice are indicated by *p<0.05; **p<0.01; ***p<0.001 (One-Way ANOVA, Tukeys post-hoc multiple comparison test). **(D)** Immunohistochemical analysis of SCRIB. Representative images at different stages of colitis (week 0, 1 & 4) are shown. Large panels: confocal z-stack images of maximal intensity projections (the scale bars are 25 µm). Inset panels: single plane confocal images (the scale bars are 10 µm).

Figure 10. Colonic expression of cell polarity proteins during the course of DSS-induced colitis in mice. mRNA expression of **(A)** *Par3*, *Par6*, *aPkcλ* and *aPkcς* (PAR complex) **(B)** *Crb3*, *Pals1* and *Patj* (Crumbs complex) and **(C)** *Scrib*, *Dlg1* and *Llgl1* (Scribble complex) in the DSS-induced colitis model (N = 10-13 mice/group (control, DSS cycle 1, DSS cycle 2, DSS cycle 3)). Significant differences between control and colitis mice are indicated by *p<0.05; **p<0.01; ***p<0.001 (One-Way ANOVA, Tukeys post-hoc multiple comparison test). **(D)** Immunohistochemical analysis of SCRIB. Representative images of control mice compared to colitis mice are shown. Large panels: confocal z-

Accepted Manuscript

Downloaded from https://academic.oup.com/ecco-jcc/advance-article-abstract/doi/10.1093/ecco-jcc/jjaa015/5718468 by Universiteit Antwerpen user on 11 February 2020

stack images of maximal intensity projections (the scale bars are 25 µm). Inset panels: single plane confocal images (the scale bars are 10 µm).

Figure 11. Discriminant analysis with mRNA expression values of *Muc1*, *Muc2*, *Muc4* and *Muc13* as predictors. Discriminant analysis for the T cell transfer and DSS models to predict healthy controls and colitis groups (week 0, 1, 2, 4, 6; DSS cycle 1, DSS cycle 2, DSS cycle 3). The main predictor variables for each function are stated in the structure matrix. (A) For the T cell transfer model, the different experimental groups were mainly discriminated by *Muc1* (function 1) and *Muc13* (function 2). Individual mice were correctly annotated to their respective groups in 57.8% of the cases. **(B)** For the DSS-colitis model, the different experimental groups were primary discriminated by *Muc2* (function 1) followed by *Muc1* and *Muc13* (function 2). Individual mice were correctly annotated to their respective groups in 69.6% of the cases.

Figure 12. Scatter plots of correlated data for the T cell transfer model and the DSS colitis model.

T cell transfer model: (A) Correlation of intestinal permeability with IL-1β protein and *Muc1* mRNA expression levels. **(C)** Correlation of *Muc1* expression with IL-1β and IL-6 protein expression. **(E)** Correlation of *Muc1* mRNA expression with the expression levels of the intercellular junctions *Cldn1* and *Ocln*. **(G)** Correlation of *Muc1* mRNA expression with the expression levels of the cell polarity complex subunits *Par3* and *aPKCζ*. **DSS colitis model: (B)** Correlation of intestinal permeability with TNF-α protein and *Muc13* mRNA expression levels. **(D)** Correlation of *Muc13* mRNA expression with TNF-α protein expression. **(F)** Correlation of *Muc13* mRNA expression with the expression levels of the intercellular junctions *Cldn1*, *Jam2* and *Tjp2*. **(H)** Correlation of *Muc13* mRNA expression with the expression levels of the cell polarity complex subunits *aPKCζ*, *Crb3* and *Scrib*. The correlations were

Accepted Manuscript

Downloaded from https://academic.oup.com/ecco-jcc/advance-article-abstract/doi/10.1093/ecco-jcc/jjaa015/5718468 by Universiteit Antwerpen user on 11 February 2020

selected based on the results of a multiple linear regression analysis. The corresponding adjusted R^2-values and p-values of the regression model are shown.

Accepted Manuscript

Downloaded from https://academic.oup.com/ecco-jcc/advance-article-abstract/doi/10.1093/ecco-jcc/jjaa015/5718468 by Universiteit Antwerpen user on 11 February 2020

Manuscript Doi: 10.1093/ecco-jcc/jjaa015

Figure 1

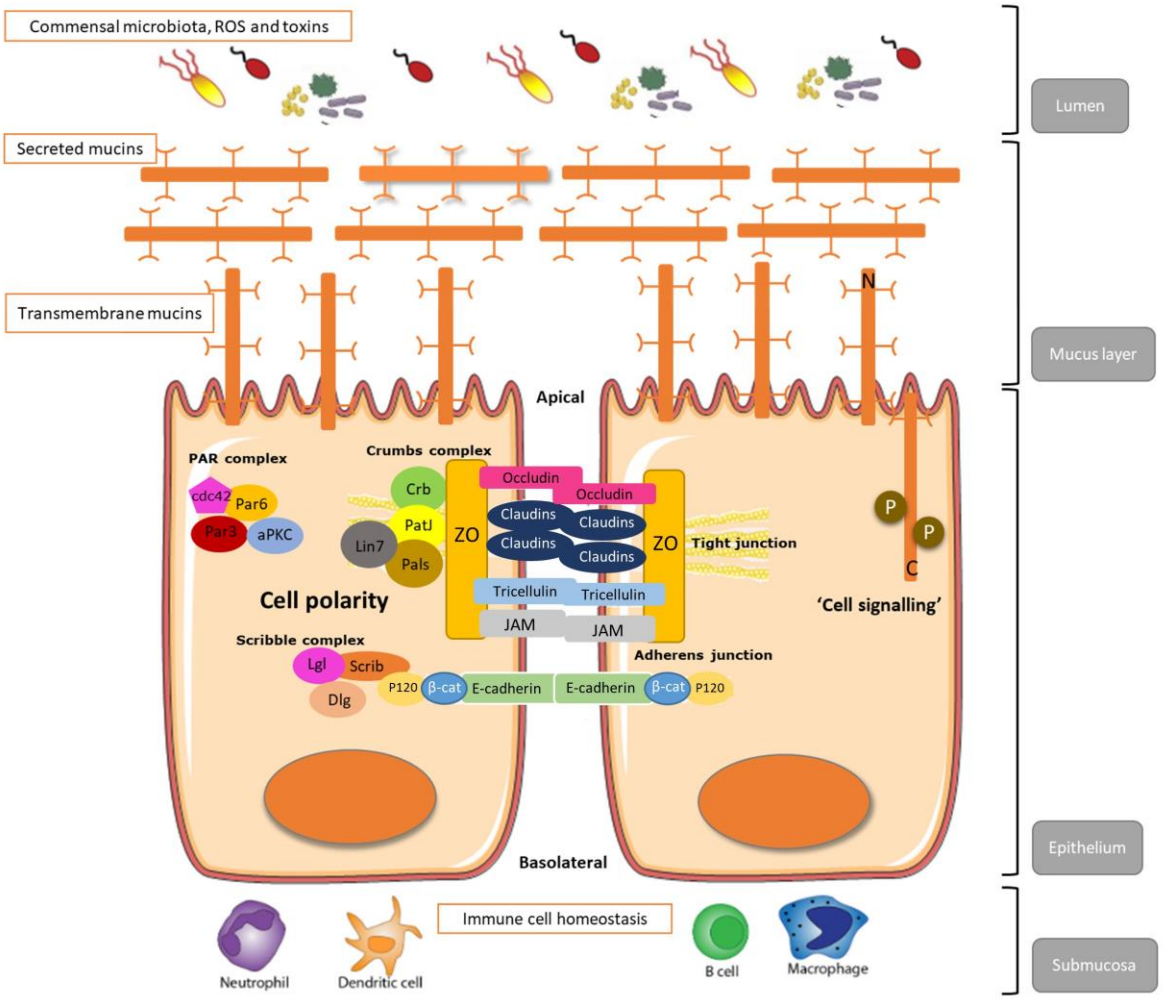

Downloaded from https://academic.oup.com/ecco-jcc/advance-article-abstract/doi/10.1093/ecco-jcc/jjaa015/5718468 by Universiteit Antwerpen user on 11 February 2020

Manuscript Doi: 10.1093/ecco-jcc/jjaa015

Figure 2

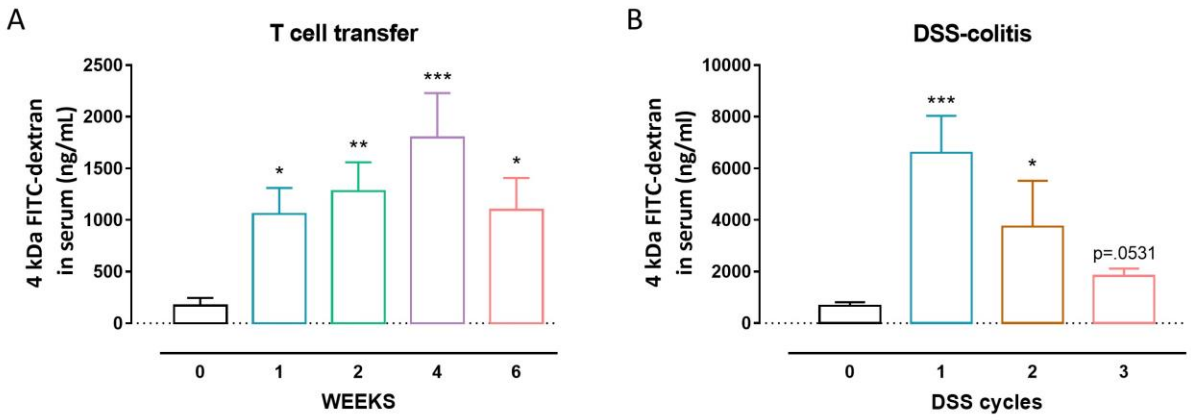

Downloaded from https://academic.oup.com/ecco-jcc/advance-article-abstract/doi/10.1093/ecco-jcc/jjaa015/5718468 by Universiteit Antwerpen user on 11 February 2020

Manuscript Doi: 10.1093/ecco-jcc/jjaa015

Figure 3

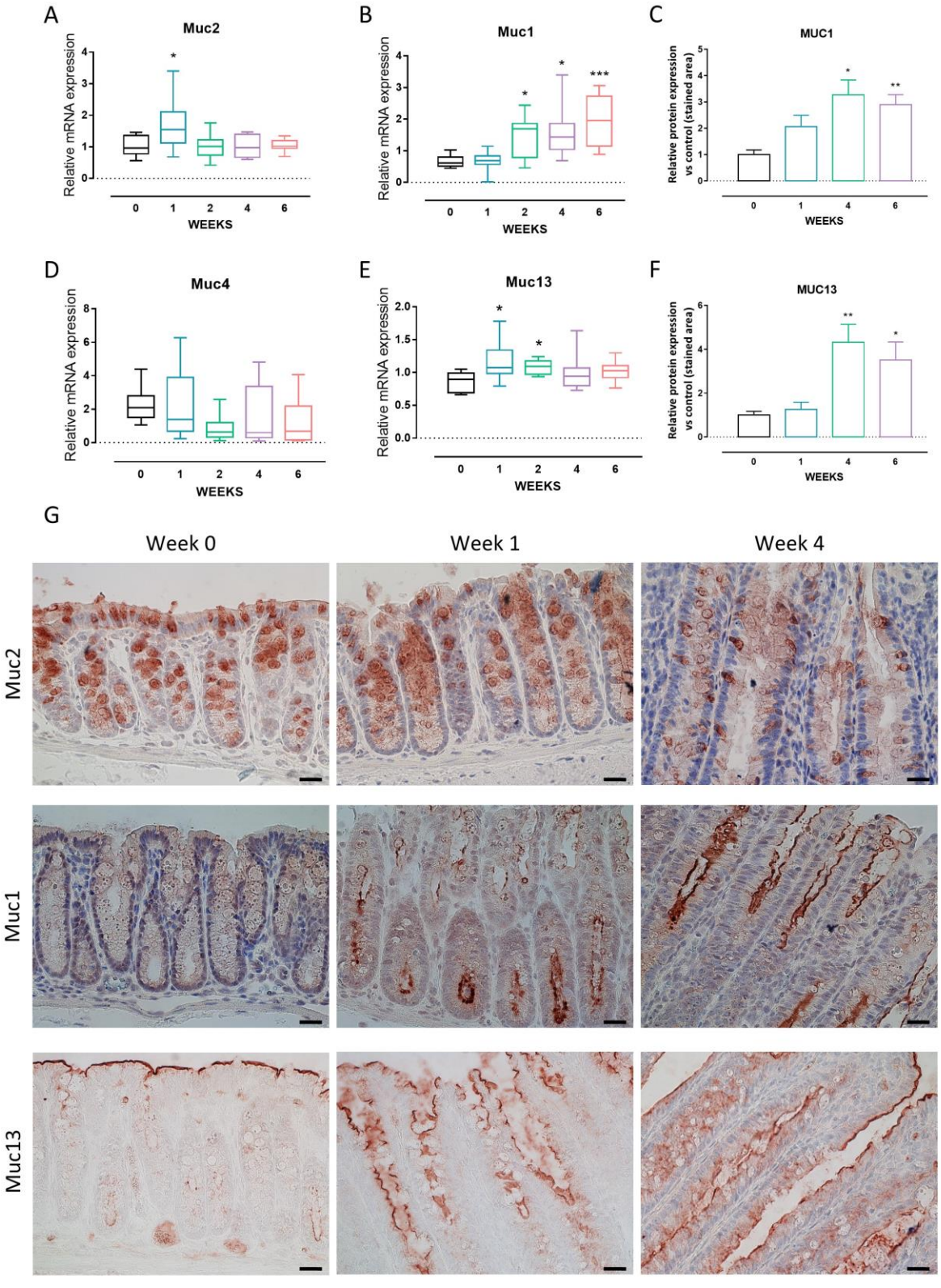

Downloaded from https://academic.oup.com/ecco-jcc/advance-article-abstract/doi/10.1093/ecco-jcc/jjaa015/5718468 by Universiteit Antwerpen user on 11 February 2020

Manuscript Doi: 10.1093/ecco-jcc/jjaa015

Figure 4

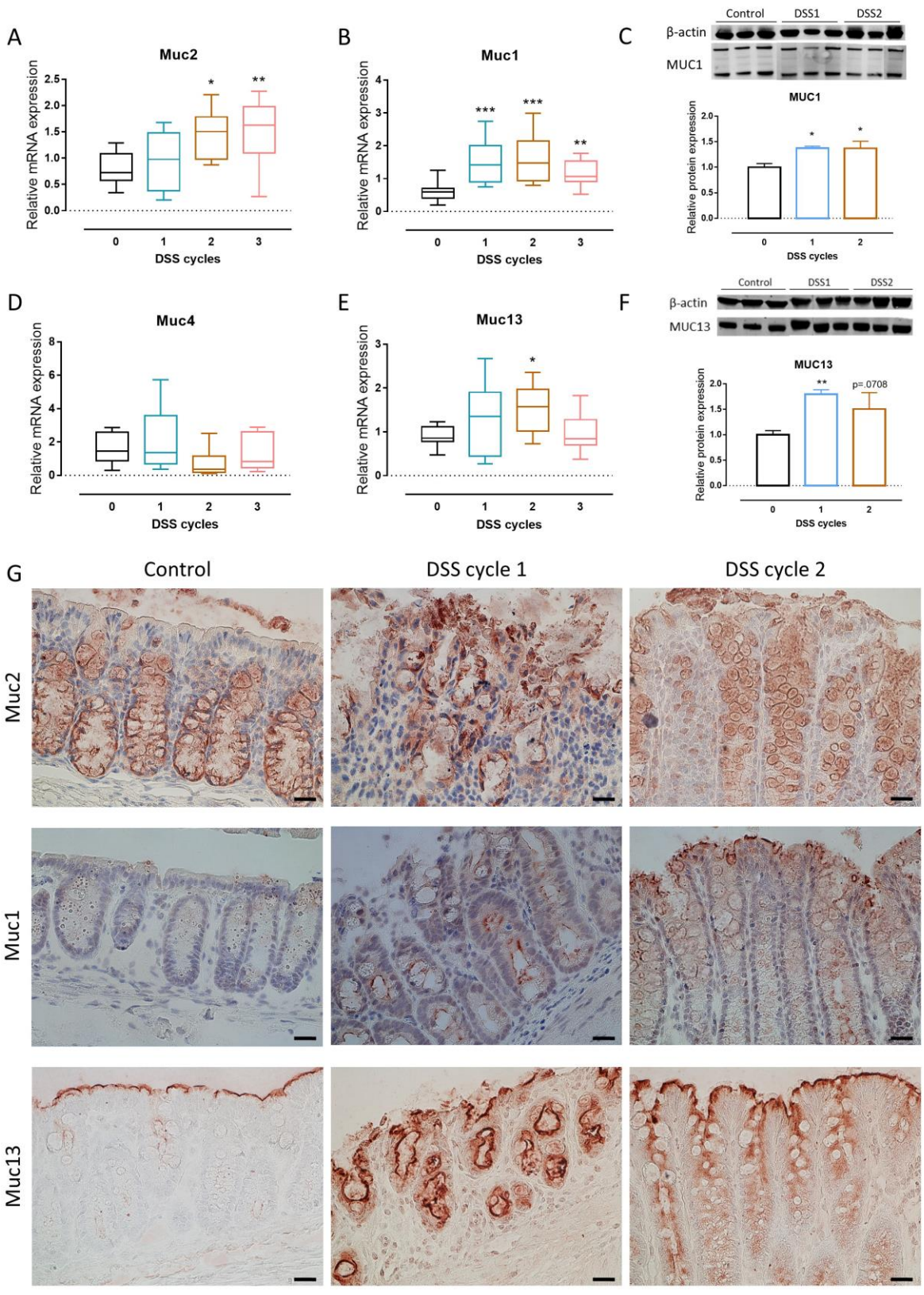

Downloaded from https://academic.oup.com/ecco-jcc/advance-article-abstract/doi/10.1093/ecco-jcc/jjaa015/5718468 by Universiteit Antwerpen user on 11 February 2020

Manuscript Doi: 10.1093/ecco-jcc/jjaa015

Figure 5

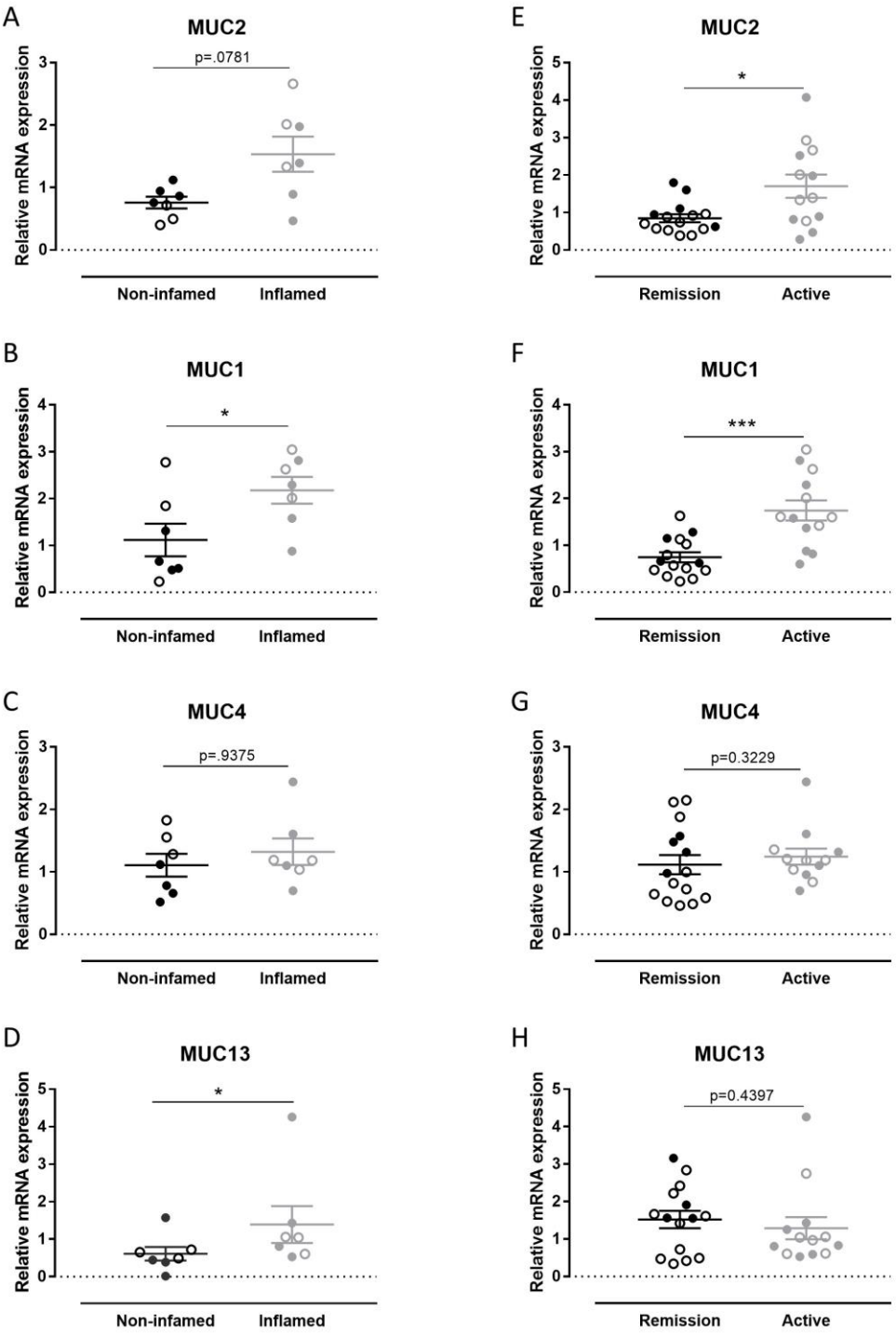

Downloaded from https://academic.oup.com/ecco-jcc/advance-article-abstract/doi/10.1093/ecco-jcc/jjaa015/5718468 by Universiteit Antwerpen user on 11 February 2020

Manuscript Doi: 10.1093/ecco-jcc/jjaa015

Figure 6

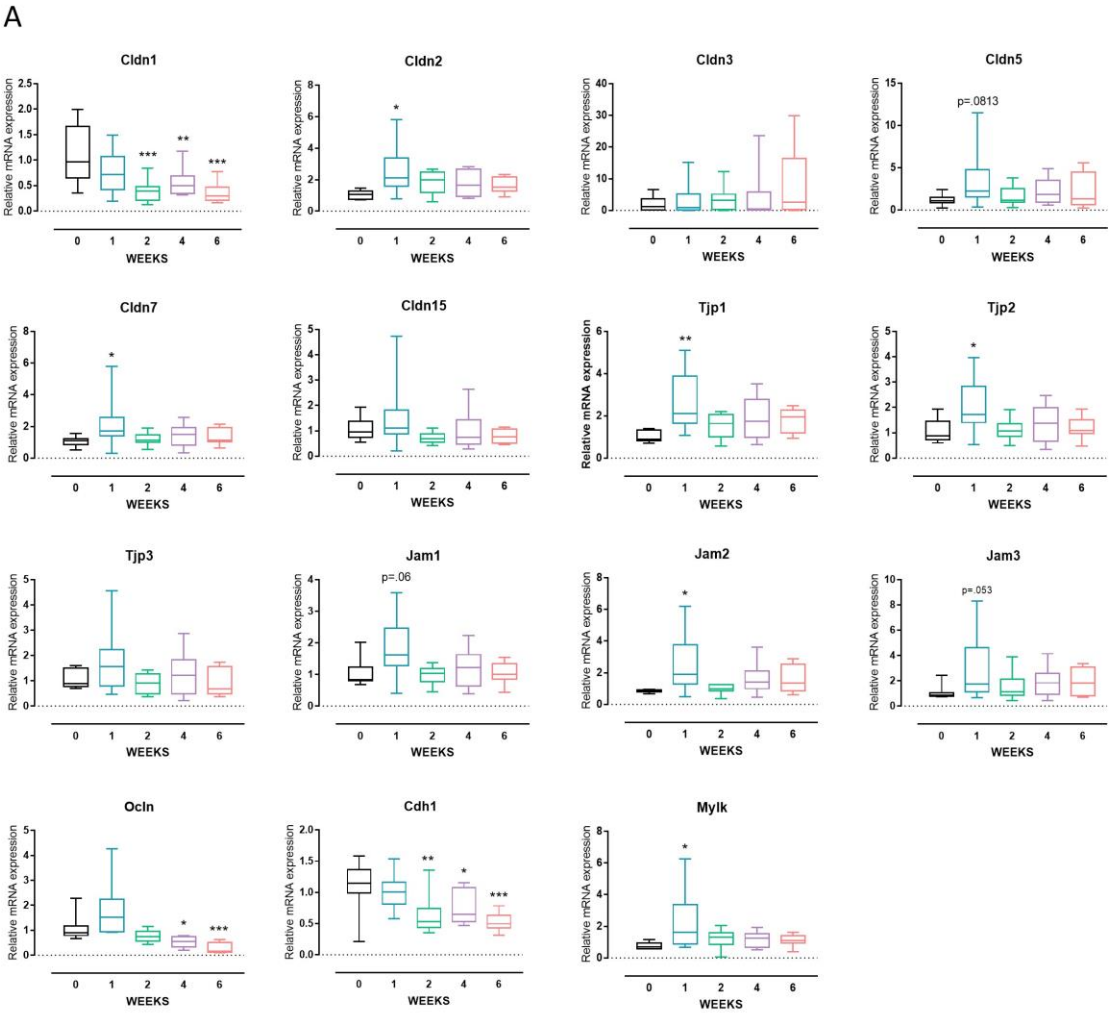

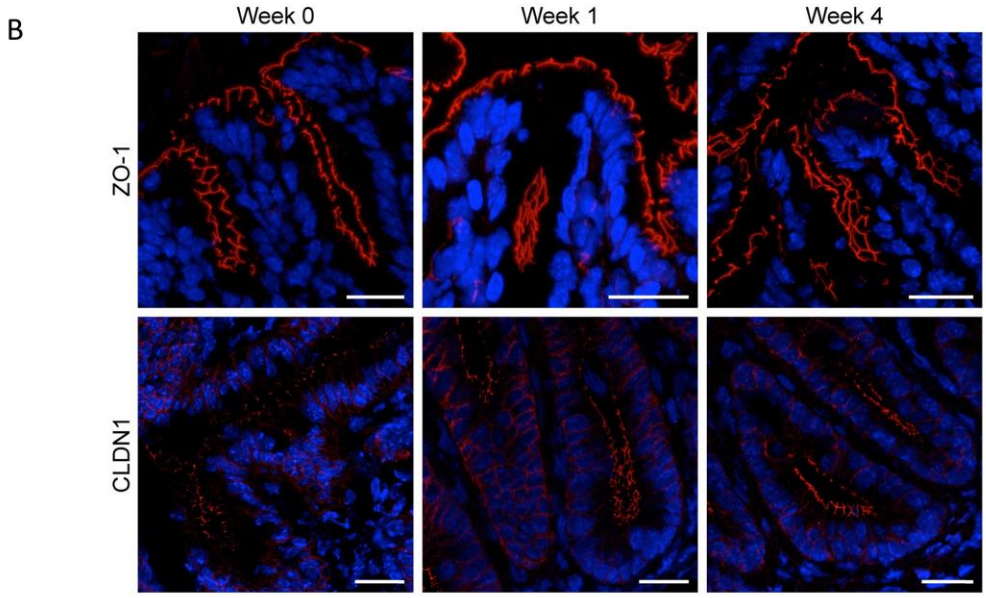

Downloaded from https://academic.oup.com/ecco-jcc/advance-article-abstract/doi/10.1093/ecco-jcc/jjaa015/5718468 by Universiteit Antwerpen user on 11 February 2020

Manuscript Doi: 10.1093/ecco-jcc/jjaa015

Figure 7

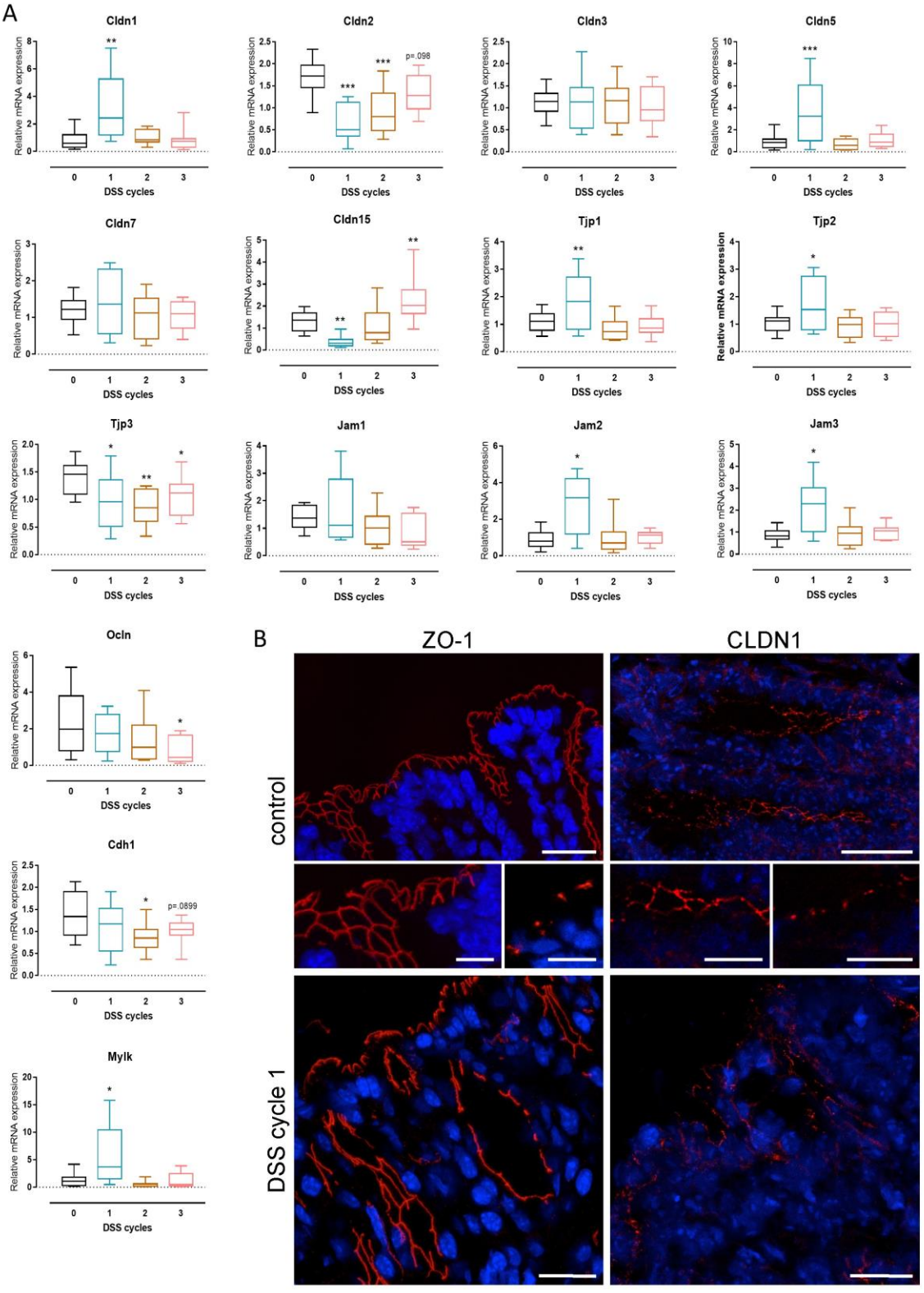

Downloaded from https://academic.oup.com/ecco-jcc/advance-article-abstract/doi/10.1093/ecco-jcc/jjaa015/5718468 by Universiteit Antwerpen user on 11 February 2020

Manuscript Doi: 10.1093/ecco-jcc/jjaa015

Figure 8

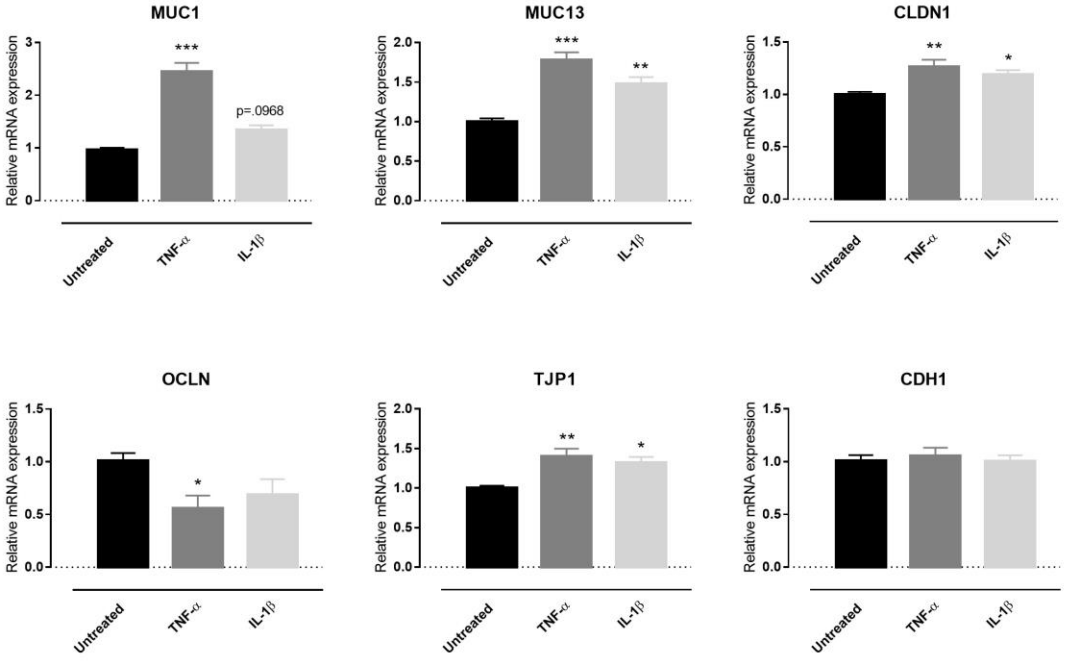

Downloaded from https://academic.oup.com/ecco-jcc/advance-article-abstract/doi/10.1093/ecco-jcc/jjaa015/5718468 by Universiteit Antwerpen user on 11 February 2020

Manuscript Doi: 10.1093/ecco-jcc/jjaa015

Figure 9

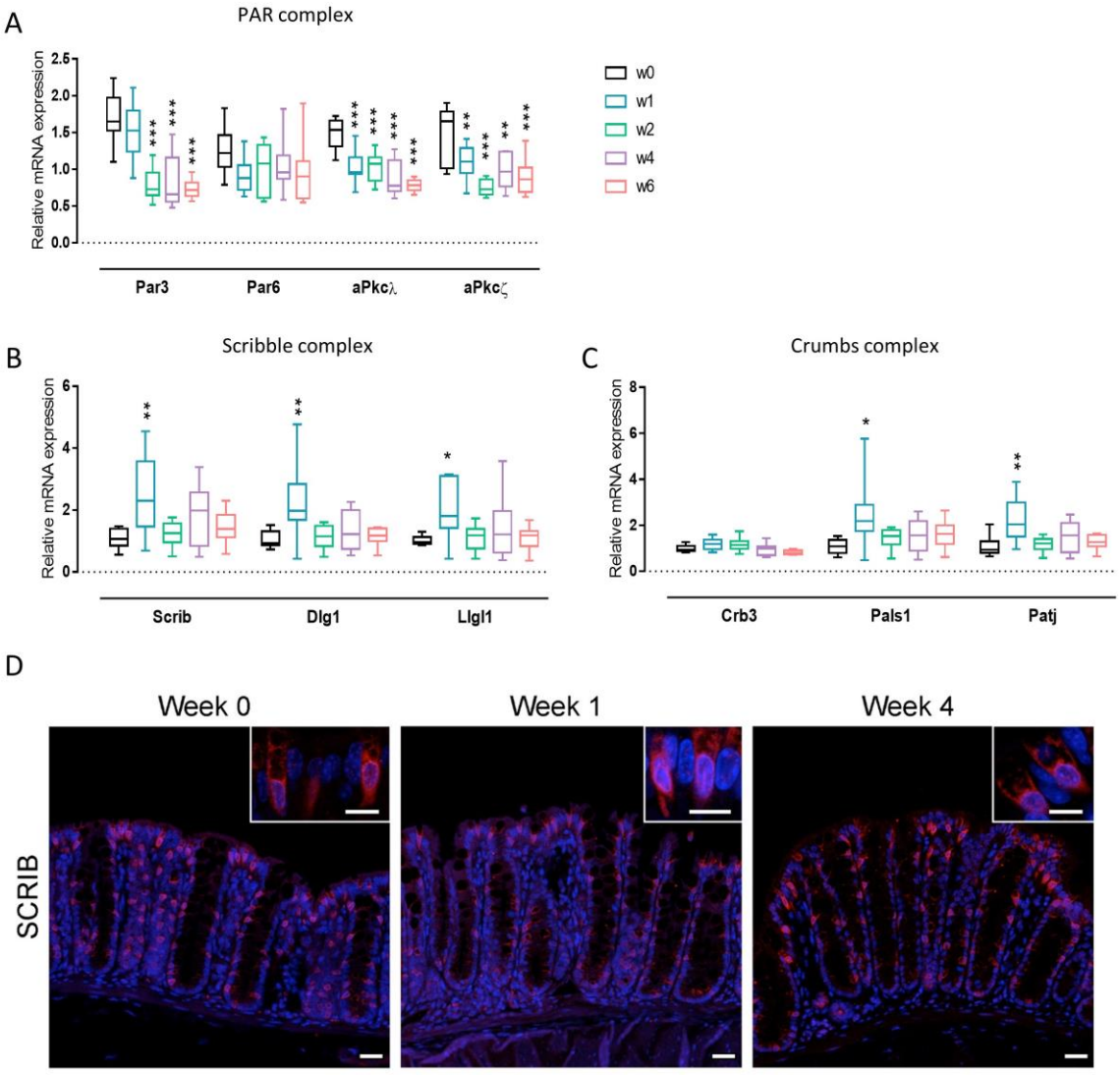

Downloaded from https://academic.oup.com/ecco-jcc/advance-article-abstract/doi/10.1093/ecco-jcc/jjaa015/5718468 by Universiteit Antwerpen user on 11 February 2020

Manuscript Doi: 10.1093/ecco-jcc/jjaa015

Figure 10

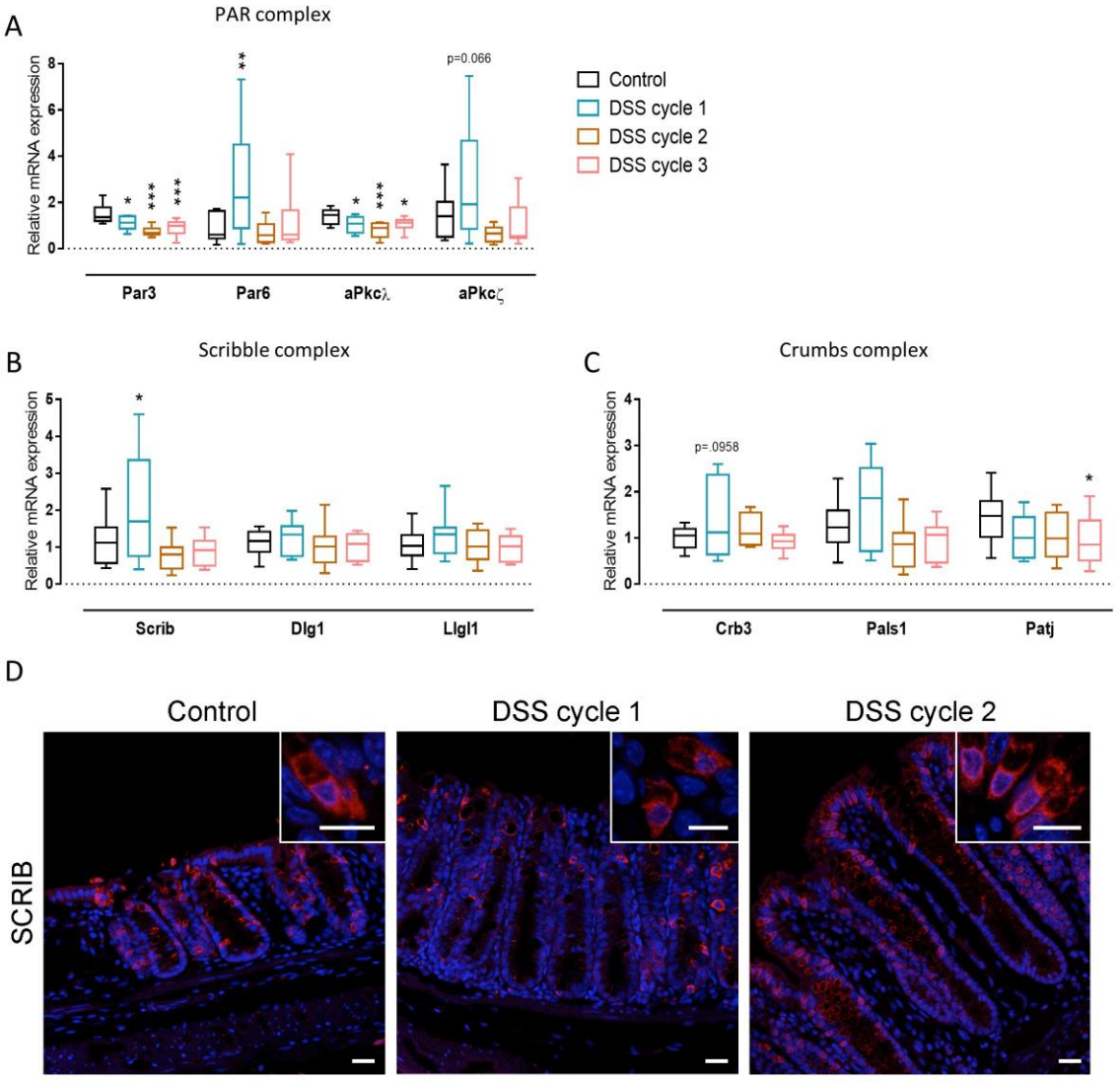

Downloaded from https://academic.oup.com/ecco-jcc/advance-article-abstract/doi/10.1093/ecco-jcc/jjaa015/5718468 by Universiteit Antwerpen user on 11 February 2020

Manuscript Doi: 10.1093/ecco-jcc/jjaa015

Figure 11

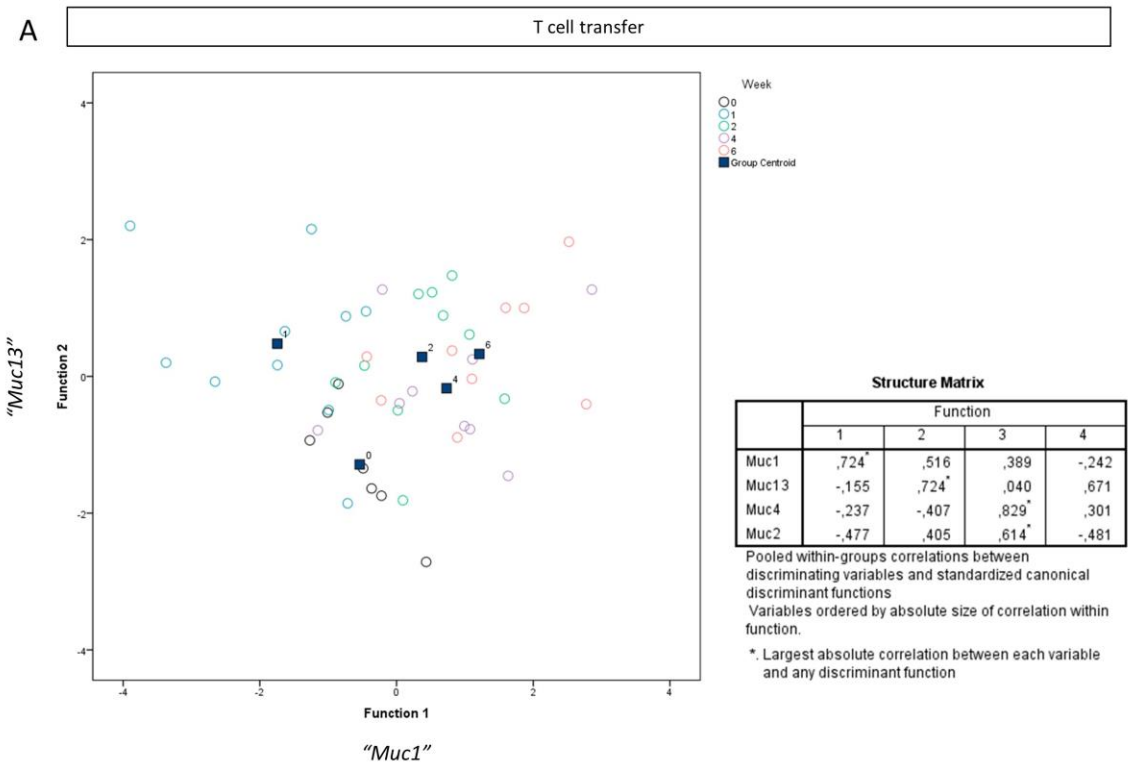

Structure Matrix

	Function			
	1	2	3	4
Muc1	,724*	,516	,389	-,242
Muc13	-,155	,724*	,040	,671
Muc4	-,237	-,407	,829*	,301
Muc2	-,477	,405	,614*	-,481

Pooled within-groups correlations between discriminating variables and standardized canonical discriminant functions
Variables ordered by absolute size of correlation within function.

*. Largest absolute correlation between each variable and any discriminant function

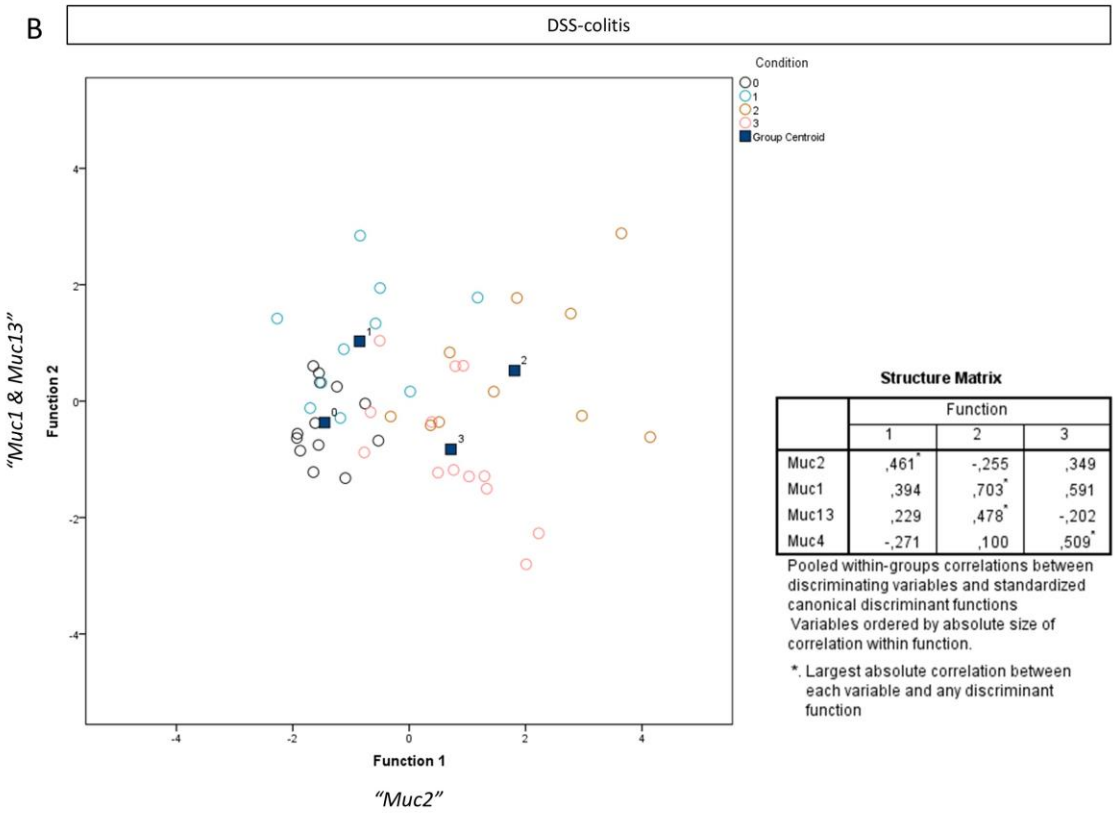

Structure Matrix

	Function		
	1	2	3
Muc2	,461*	-,255	,349
Muc1	,394	,703*	,591
Muc13	,229	,478*	-,202
Muc4	-,271	,100	,509*

Pooled within-groups correlations between discriminating variables and standardized canonical discriminant functions
Variables ordered by absolute size of correlation within function.

*. Largest absolute correlation between each variable and any discriminant function

Downloaded from https://academic.oup.com/ecco-jcc/advance-article-abstract/doi/10.1093/ecco-jcc/jjaa015/5718468 by Universiteit Antwerpen user on 11 February 2020

Manuscript Doi: 10.1093/ecco-jcc/jjaa015

Figure 12

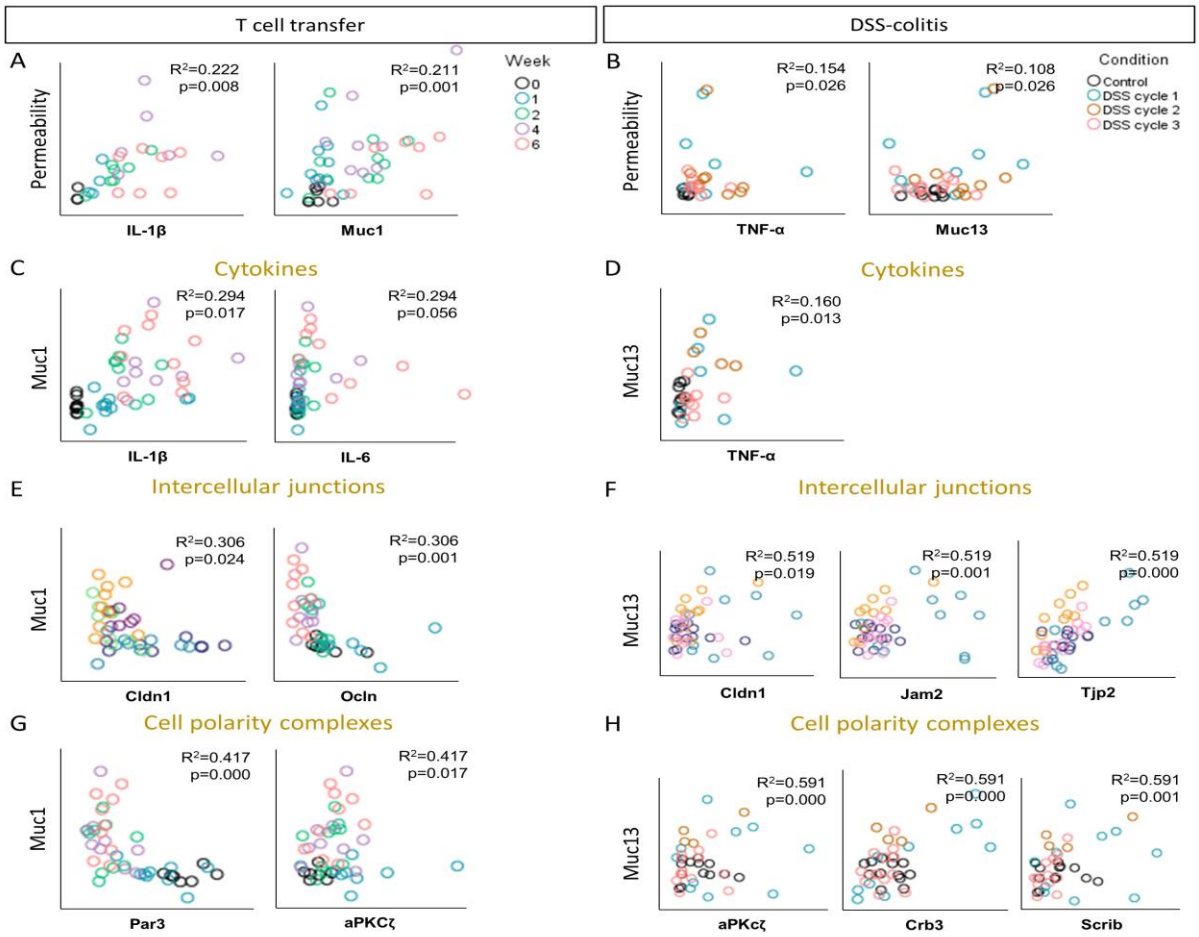

Downloaded from https://academic.oup.com/ecco-jcc/advance-article-abstract/doi/10.1093/ecco-jcc/jjaa015/5718468 by Universiteit Antwerpen user on 11 February 2020